Design of an Unmanned Aerial Vehicle

by
Jean-Marc C. Hauss

B.S. Mechanical and Aerospace Engineering
& B.A. Physics
Cornell University, 1997

Submitted to the Department of Aeronautics and Astronautics in partial fulfillment of the requirements for the degree of

Master of Engineering

at the
Massachusetts Institute of Technology

June 1998

Author _____
Department of Aeronautics and Astronautics

Certified by _____
Charles Boppe
Senior Lecturer, Department of Aeronautics and Astronautics
Thesis Supervisor

Accepted by _____
Jaime Peraire
Associate Professor
Chairman, Department Graduate Committee

Design of an Unmanned Aerial Vehicle

by
Jean-Marc C. Hauss

Submitted to the Department of Aeronautics and Astronautics on 22 May, 1998, in partial fulfillment of the requirements for the degree of Master of Engineering

Abstract

Information gathering is becoming one of the growing assets for the military in combat situations. America's vast intelligence network provides it with a way to quickly and efficiently perform sensitive military exercises. One area lacking in this domain is in rapidly obtaining information on events happening not far from the frontline. For instance, today's military commander would have to go through far away bases to obtain information on the location of enemy troops that are a few miles away.

One of the main objectives of the project behind this thesis was to provide the US Armed Forces and more specifically the Navy with a quick, cheap way to perform visual, short range reconnaissance missions. The concept is to launch an artillery shell containing a miniature unmanned aircraft right over the desired location. The advantage of this concept is that a reconnaissance mission can be done quickly, at low cost, and without requiring any landing strip. Major considerations in obtaining such a product are the high impulse forces affecting the aircraft during the artillery launch, and having to package a fully deployable aircraft inside a size-constrained shell.

Thesis Supervisor: Charles Boppe
Title: Senior Lecturer, Department of Aeronautics and Astronautics

Acknowledgments

I would first like to thank Draper Laboratory for giving me the opportunity to take part in this project. It is not common for a group of students to be able to take part on such a large project. This has been a very beneficial learning experience for someone about to embark into industry.

I would also like to thank professors Deyst and Boppe for their help and guidance throughout the year.

I also thank the team and especially its manager Sebastien Katch for having taught me the art of making an acceptable technical drawing.

Finally, I thank my parents and my brother for supporting and encouraging me in these past few years.

Table of Contents

List of Figures

List of Tables

Introduction

This thesis serves as an overview of the work done by the WASP (Wide Area Surveillance Projectile) team on the design of a surveillance projectile. It will describe, in greater details, the work done by the author.

The first chapter will give a background of the project and how it came about. It will also go over the work performed in the first year of this two year project. It briefly describes how the concept of a gun launched unmanned aircraft was selected.

Chapter two gives a more detailed description of the technical aspects of the project. It includes the different tests used to demonstrate the validity of the design. This chapter discusses the different project components. An overview of the author's work on the project is then provided.

The next three chapters go into details describing the author's part of the project. Chapter three describes how the power systems for the different vehicles were designed. Chapter four goes over the system selected for the tail actuators. Chapter five looks into the backup plan for the propulsion system.

Chapter six goes over all the testing results for the different parts of the project. The results for the final system testing are also included.

Chapter seven discusses the conclusions and the lessons learned for the project.

1.1 MIT-Draper Partnership

The project behind this thesis is funded and supervised by Draper Laboratory. The association between Draper Laboratory and MIT is long-standing as Draper Laboratory initially was an integral part of MIT. The MIT/Draper Technology Development Project was created in the Summer of 1996 to consolidate this cooperation between Draper and MIT's Aeronautics and Astronautics Department.

About ten students were to work on a project for two years. There were five Master of Science students and another five Master of Engineering students, with a few undergraduate UROPs helping out. The Master of Engineering is a one year program. Two different sets of MEng students worked on the project. Being one of those Master of Engineering students, the author joined the team for the second year.

1.2 Project Goals

The project's main requirement was to design a nationally important aerospace system in two years time. One of the project's characteristics is that it had to include a high level of "unobtainium," or a high level of risk. For the first set of students working the first year, the initial task was to come up with a set of projects satisfying these requirements and perform a feasibility analysis. This was done during the first six months of the project. Figure 1 shows the tasks performed for this first part.

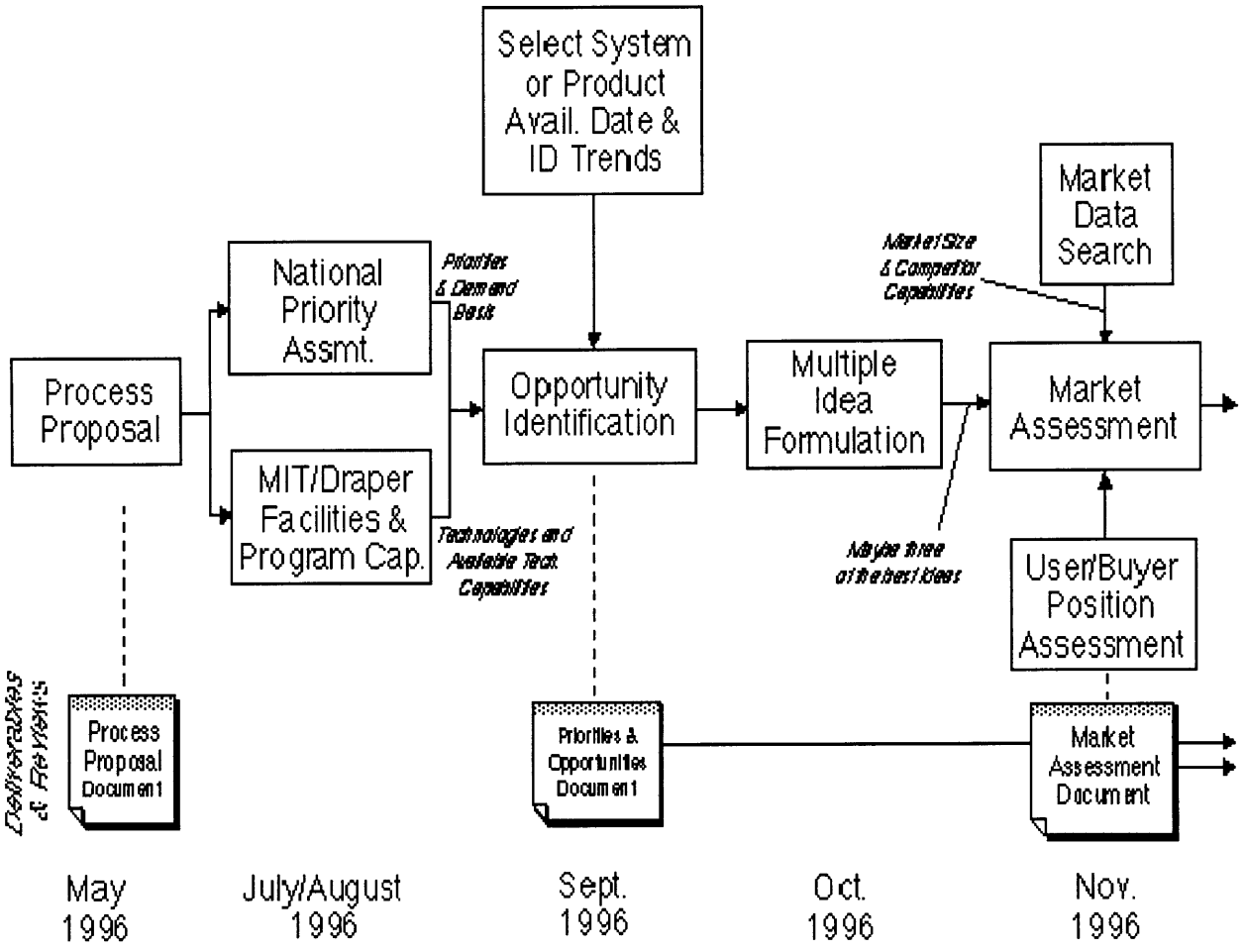

Figure 1: Sequence of Events Leading to a System Selection

At this point, the fast response surveillance projectile was selected. This marks the beginning of WASP. During the next six months, the team came up with different concepts for the flyer. The final concept chosen was that of a vehicle fitting inside an artillery shell. This marked the end of

the work for the first year students. At this time, the second set of students, joined the project team. In the first six months of the second year, the detail design of all the different components was performed. Finally, the last six months comprised experimental testing of all the parts, and putting together all the components into a system. The sequence of events for the second part of the project, the design of WASP, can be seen in figure 2.

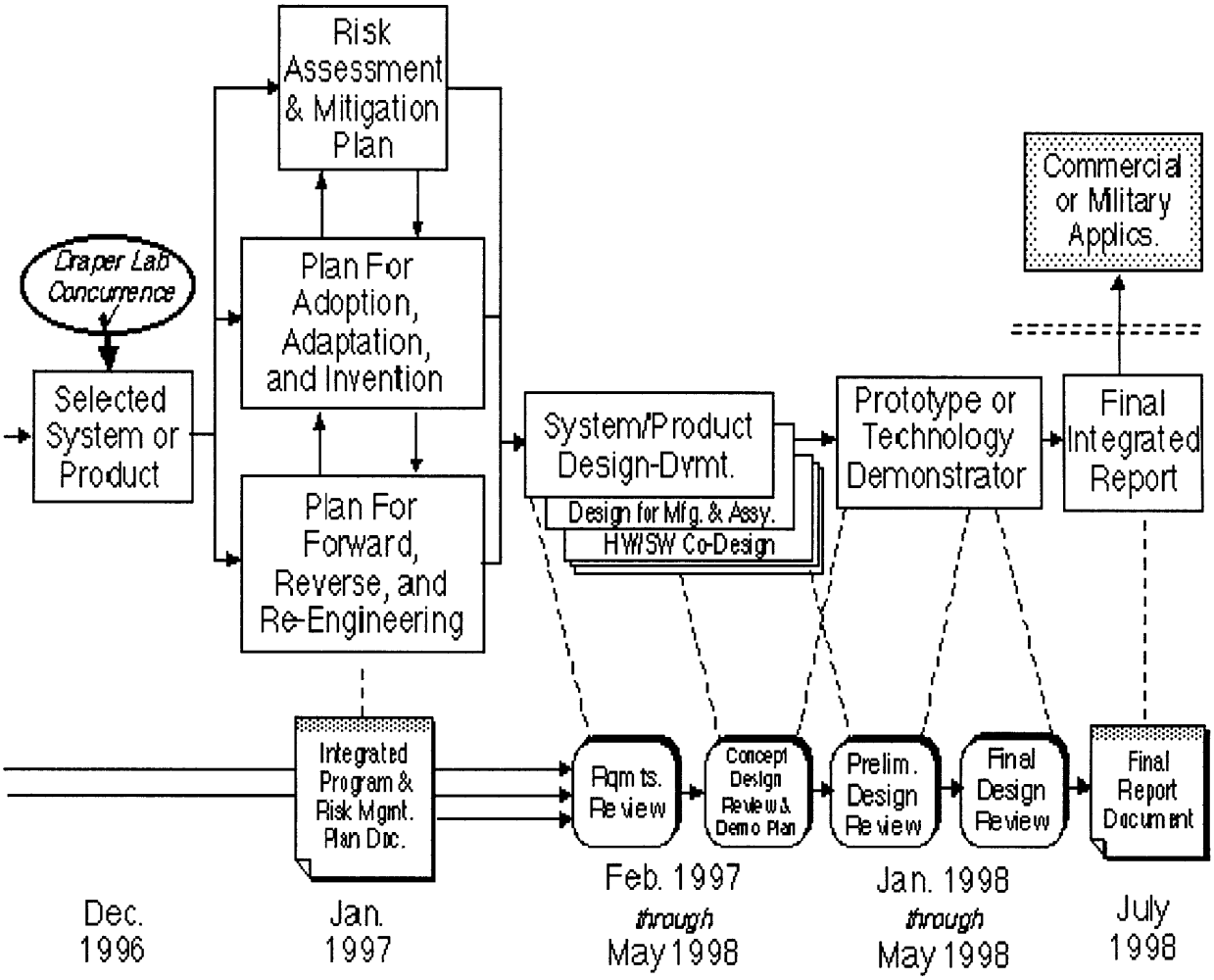

Figure 2: Sequence of Events for Concept Design and Development

The final objective was to come up with a working prototype demonstrating the feasibility of the concept.

1.3 Work Performed during First Year

First year work consisted mostly of selecting a system to design, and an initial analysis of the feasibility of this design.

The team first looked at different concepts that fit the requirement to design a high risk prototype satisfying a national need. Some of the concepts considered were a solar sail, a search and rescue vehicle, and a method to send vehicles into orbit by launching them from the high atmosphere. As discussed, the final concept selected was a rapid response vehicle that could provide short range reconnaissance. The system's benefits were that it would provide a reconnaissance capability in a short amount of time, and could do it for a fraction of the cost of existing systems.

To provide a rapid response, the projectile would be launched from a gun. Different concepts were then considered. Some of the options were to use a composite shell, have a sabot protect the flyer when inside the gun, or have the flyer inside an artillery shell until it is to be deployed. This last option was chosen.

Another important task completed during the first year involved selecting what technology should be used to perform different functions in the final vehicle. This consisted of an analysis of different ways to perform different operations. For example, an analysis was performed on how to propel the flyer. Rockets, gas engines and electric motors were all considered as candidates. By analyzing the advantages and disadvantages of each mode of propulsion, the gas engine was selected. Another such analysis was performed on how to stow the flyer's wings before being deployed.

Project Description

The goal of the project was to design a fast-response reconnaissance unmanned aircraft. The underlying method is to fit the aircraft inside an artillery shell. This chapter gives a description of the project as a whole and where the author's responsibilities lie.

2.1 General Project Description

2.1.1 Concept Description

2.1.1.1 Typical Mission Scenario

With the work performed during the first year of the project, a relatively accurate mission scenario was obtained. This description of a typical scenario will give a good feel of what this project is about. The following description represents the project as it stood when the author joined the team in September 1997. As aforementioned, the vehicle is initially inside a five inch Navy artillery shell and is stored that way until it is to be used. The shell is fired at the request of the ship's captain or battalion commander. As the projectile exits the gun barrel at 680 m/s, fins located at the back of the shell deploy to allow for a stable projectile. Then somewhere around the peak of the trajectory, the back part of the shell separates with an explosive bolt. Shortly thereafter, a parachute is deployed to decelerate the vehicle from 340 m/s to around 50 m/s. The parachute also has the effect of removing the flyer from the surrounding shell. Once the vehicle is outside the shell, a propeller driven by an engine starts, two foldable wings deploy and two tails deploy. Once the vehicle is a deployed flyer, the engine and the electronics are started. From here, the aircraft flies on its own and takes pictures which are relayed back to a ground station. An illustration of this sequence can be found in figure 3.

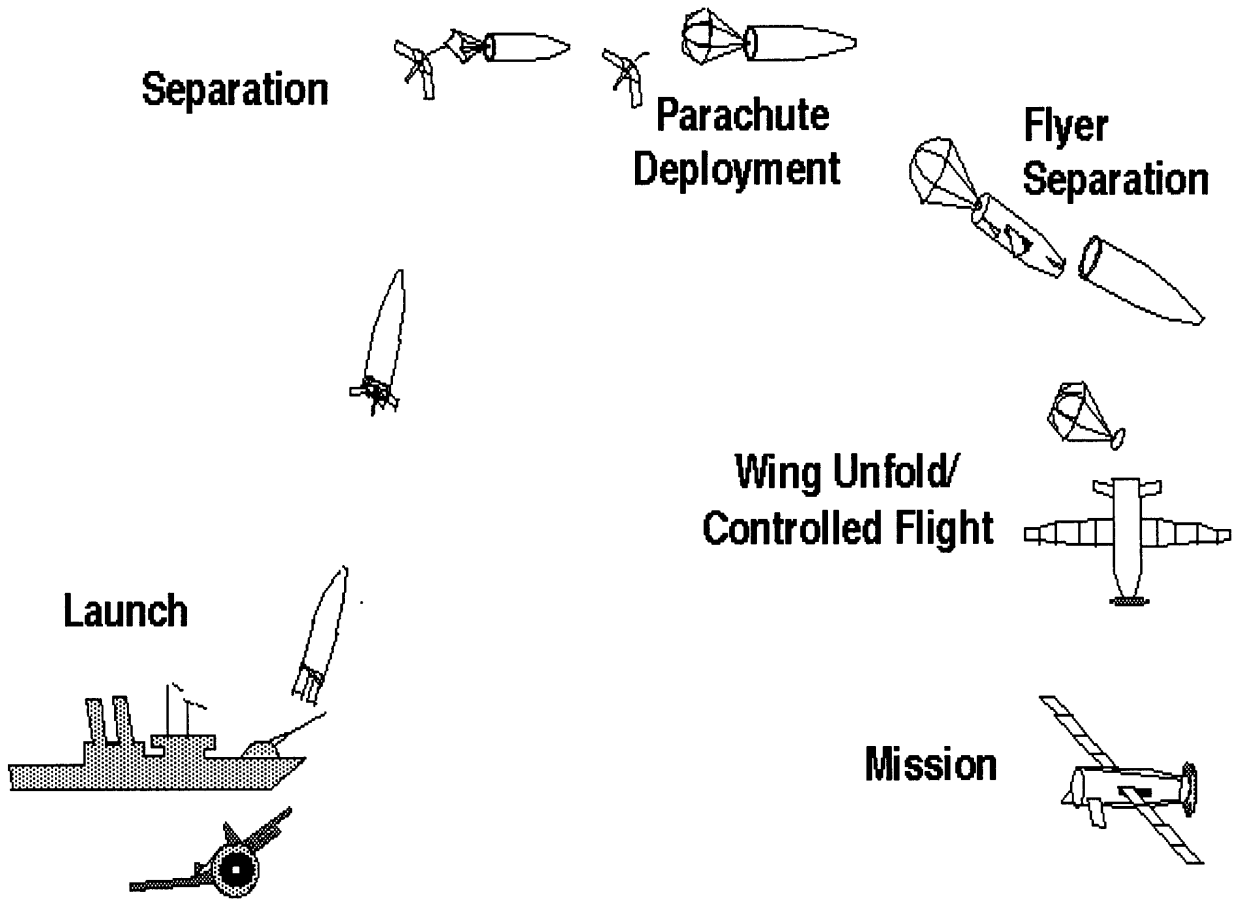

Figure 3: Deployment Sequence

This represents the backbone of a typical scenario. Different considerations were taken to allow for different missions. For instance, the parachute could be deployed at different times, or the plane could perform different search patterns from its deployed state.

2.1.1.2 Design Challenges

The major technical requirement was to design a vehicle that could withstand the initial artillery launch. This initial force can be separated into different components. First there is the forward axial acceleration which is a seventeen millisecond pulse of 15000 g's. This is the largest force and hence the one given the most consideration. Then there is a backwards axial acceleration represented by a shorter pulse of 4000 g's, called setback. This comes about from the compression of the shell under the initial acceleration. The rear of the shell accelerates faster than the

front which compresses the shell. Finally there is a radial vibration with a peak amplitude of 1000g's. This comes from the spinning of the shell inside the gun barrel. This g-loading requirement applies to the whole vehicle and was a major concern.

Another main design challenge is to have all the components fit inside a standard military shell which is the five inch shell in the case of this flyer. The five inch shell was chosen since it is the one used most often by the intended customer, the Navy. This means that the flyer has to be even smaller than the five inch diameter, two feet long shell. Everything from the wings to the propulsion system and the electronics have to fit inside this small volume.

These requirements make for a state-of-the-art design problem with nothing of the sort ever having been done. Some projectiles using the concept of firing something inside an artillery shell have already been designed. For instance, there exists an illuminating round which is used to illuminate a battle field. This is basically a flare inside an artillery shell which is fired, deploys, and then slowly descends while being held up by a parachute. Ideas from this design, such as the design for the back of the shell were used. But this design comes nowhere near the complexity of having a small scale aircraft deploying from a shell.

2.1.2 The Proof of Concept Test Vehicles

The demonstration of the functionality is done by performing two types of tests. For all the structural and flyer separation demonstration there is the high-g test. For the avionics and aerodynamic performance, there is the Flight Test Vehicle. These two series of tests are then put together into the operational vehicle, which is the final working vehicle (figure 4). This operational vehicle is only a paper design because most of the high-g qualified electronics were still unavailable at the time of the design.

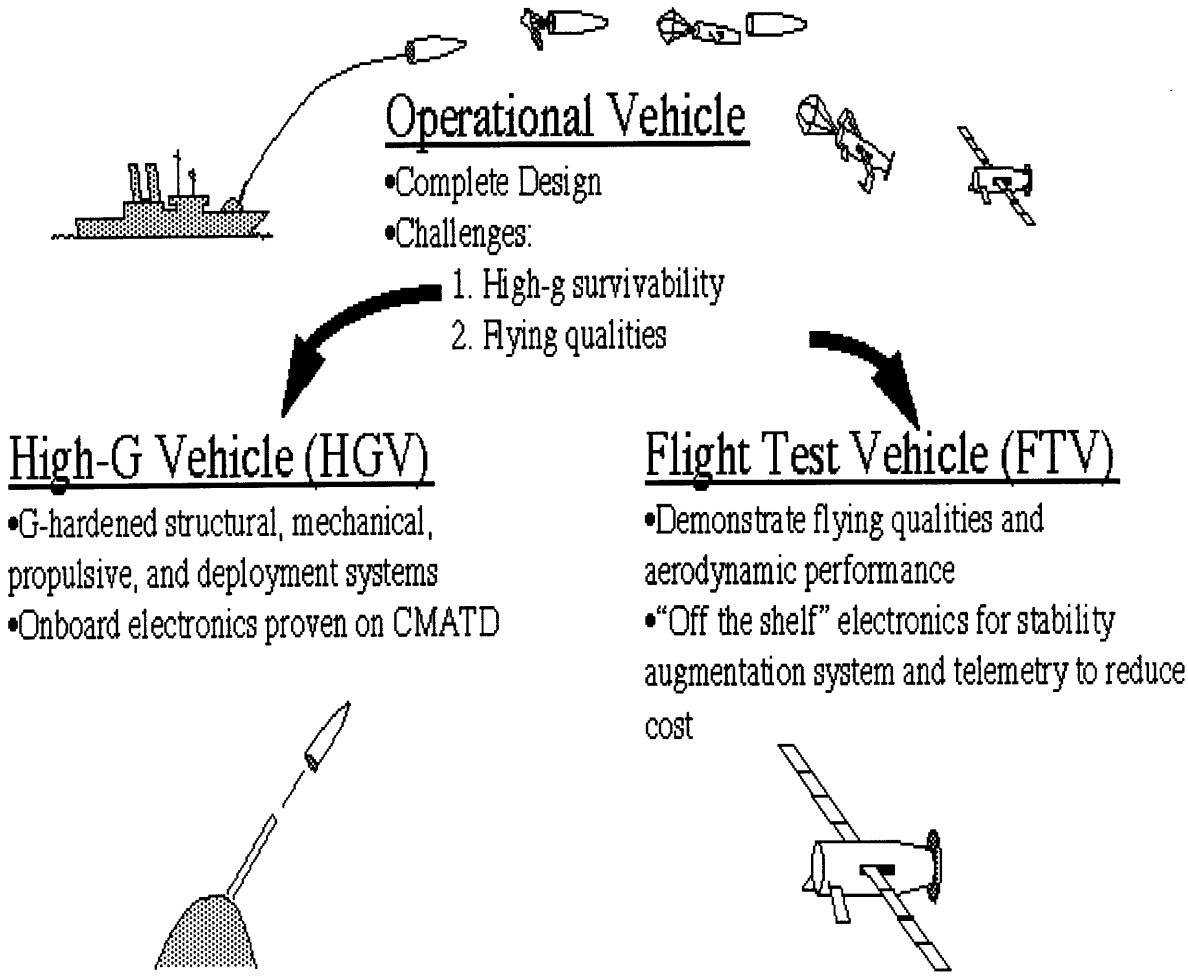

Figure 4: Concept Demonstration

2.1.2.1 High-g Test Vehicle

The high-g test vehicle is used to verify the structural response of the operational vehicle under the gun launch. It is also supposed to verify all the separation mechanism. This includes extracting the flyer out of the shell, deploying the wings, and starting the engine. First there is a series of high-g tests for individual components to see if they can withstand a gun launch. To this extent, the Air Gun at Picatinny Arsenal in New Jersey was used (figure 5).

Figure 5: Air Gun at Picatinny Arsenal

The air gun can give the 15000 g's with a two ms pulse. This isn't identical to the real Navy gun characteristics. The Navy gun has about a seventeen milliseconds pulse and in addition gives the 4000 g set-back acceleration which isn't felt in the Air Gun. Nonetheless the Air Gun was used since the cost is $1000 per test compared to around $40000 for the real gun. In addition, since the project is performed by a university, the team was able to secure twenty-eight of these tests for free. For this series of tests, the component to be tested is placed inside a specific canister (figure 6) that fits inside the Air Gun. The typical procedure is to test an article at different accelerations. To this extent each test article would usually be tested three or four times, starting at accelerations around 5000 g's and slowly increasing the acceleration to about 15000 g's.

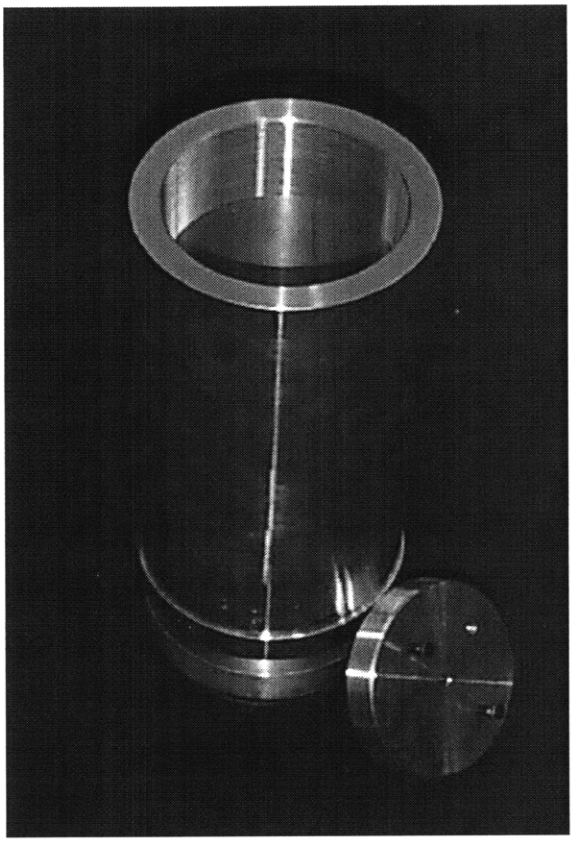

Figure 6: Air Gun Canister

A second series of tests would be used to verify the separation sequence. There are a few options for this. A drop test could be performed where the shell is dropped and the separation is performed at the right speed. Another option is to fire a real shell to verify the separation. At the time this thesis was completed, these tests had been deferred, mostly because the separation required the use of explosives. The team had difficulties obtaining the services of professionals qualified to handle explosives.

All of these tests are combined to verify the system as a whole. At first, the plan was to have the whole flyer, without the avionics, put inside a shell and fired from the real gun. The goal was to have the flyer come out of the shell and fly. No pictures were to be taken and the avionics weren't supposed to be included since none of these components would be available in g-hardened form. Eventually because of costs, and concerns with the explosives to be used in the

deployment sequence, this test would be scaled back to a canister test in the real gun. The advantages of this test relative the air gun tests were that the real gun acceleration would be felt by the flyer, and the whole assembly would be tested.

2.1.2.2 Flight Test Vehicle

The Flight Test Vehicle (FTV figure 7) is supposed to test everything that could not be tested in the high-g environment. This includes the aerodynamic performance, the stability augmentation, the unmanned vehicle aspect and taking pictures with the camera. To that extent the FTV is an aircraft similar to the final operational vehicle that is not high-g qualified. At first, the aircraft will be a remote controlled aircraft commanded by a ground based pilot. This will allow for the testing of the aerodynamics and stability augmentation. Once this is done, the aircraft will no longer be controlled by the pilot but by the on-board CPU. This will prove the un-manned aspect. Finally, the camera will be integrated and will relay the pictures taken back to a ground station. This is to prove the ultimate functionality of the flyer.

The FTV is a 128% scaled up version of the final vehicle because some of the avionics, such as the IMU selected, could not fit inside the real vehicle. This scaling was done while keeping all the important aerodynamic characteristics identical.

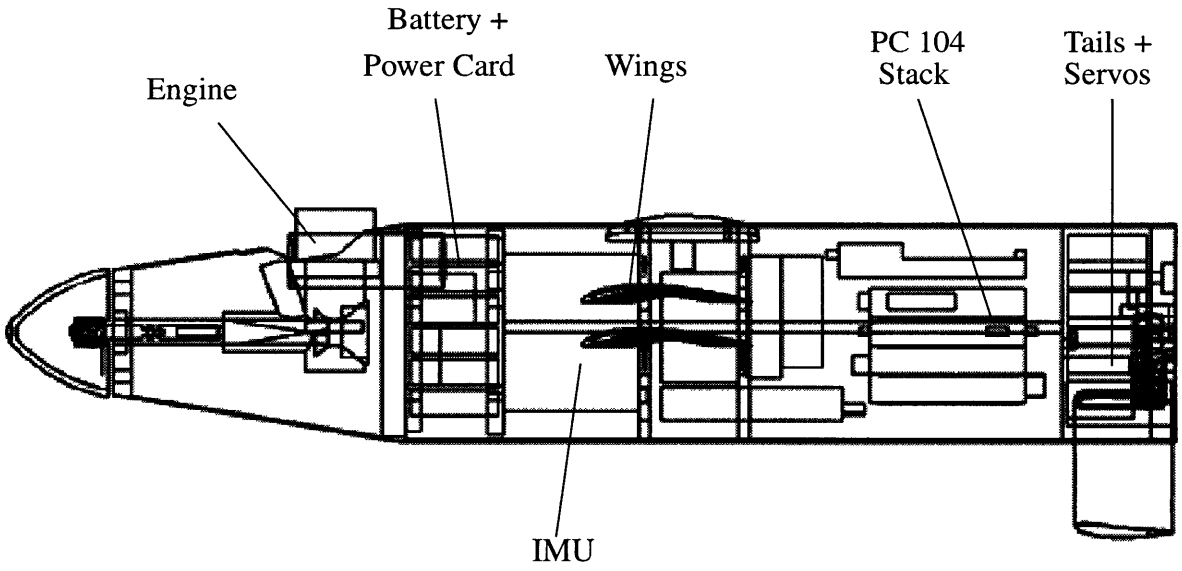

Figure 7: Configuration of FTV

Figure 8 shows how the FTV will operate. There are two ways to control the aircraft. Either the pilot sends the command to the aircraft through the transmitter, or the aircraft is controlled by the on-board computer. An FPGA chip allows the pilot to toggle between these two control modes. There are three actuators that allow for the control of the aircraft. There are the two tail servos and the engine servo. All of this is very similar to what is supposed to happen on the final operational vehicle. The main modification is the use of a transmitter and the FPGA chip. In the operational vehicle, all commands are given by the computer, and there is no pilot.

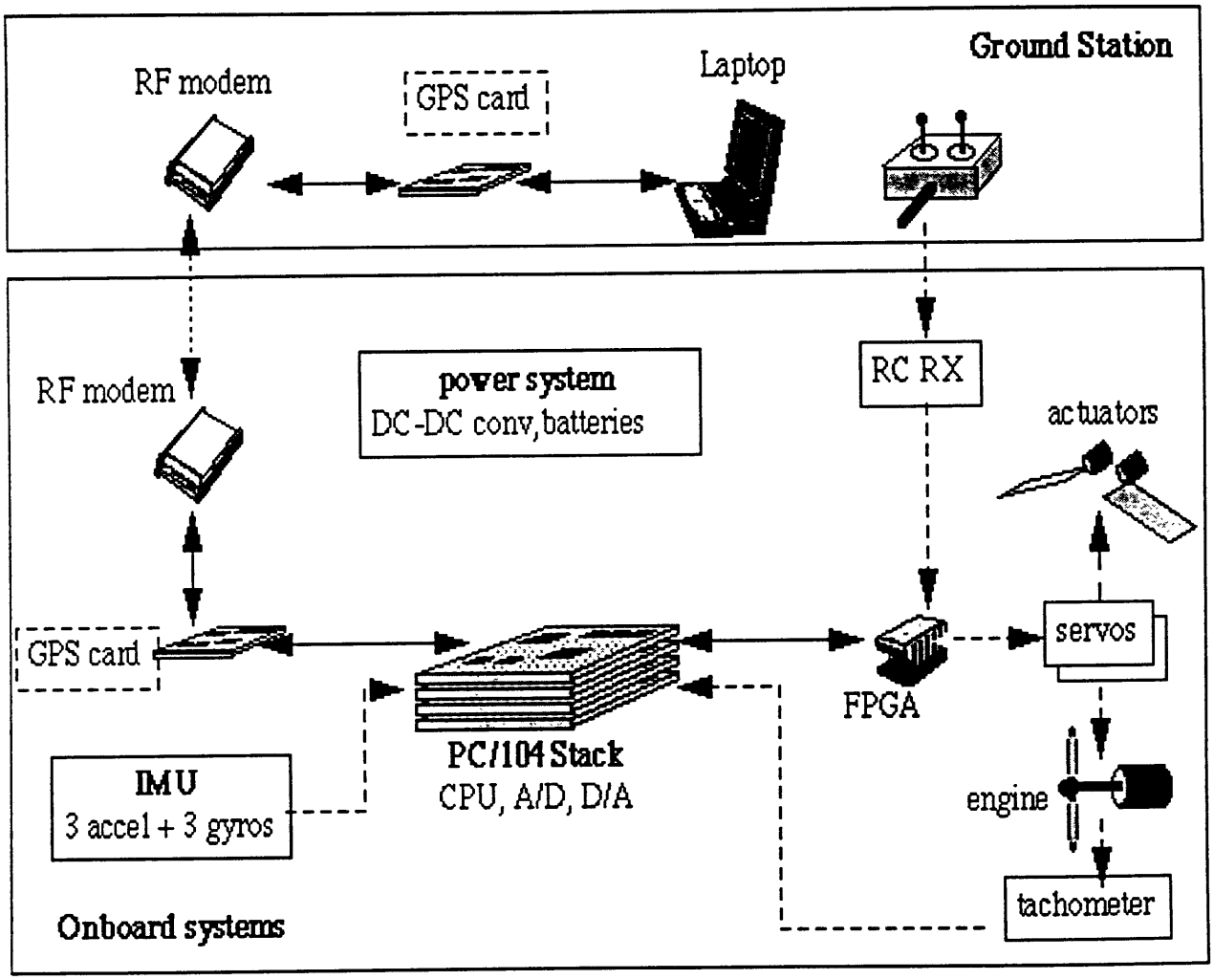

Figure 8: Control Architecture of FTV

2.2 Team Breakdown

The work was broken down according to parts of the design. One big part dealt with the back part of the shell. This part comprises work on the parachute, the retrieval of the aircraft from the shell, and the stabilizing tail fins. Another part is designing the wings. This includes the aerodynamics as well as the folding mechanism. Next, there is the propulsion system which comprises designing the engine and everything that comes with it (starter, gas tank, glow plug and propeller deployment). Another important section is the stabilization of the aircraft and the avionics that comes along with it. Finally everything has to be put together, meaning that some sort of internal structure of the aircraft had to be designed. Each of these sections were assigned to specific teams. The break up of the work lead to the modularisation of the vehicle, with a certain section of the vehicle being assigned to different teams. This allowed the teams to move ahead with their designs without being affected too much by the design changes of some other part. These different parts are described hereafter in more detail.

2.2.1 Back-End Module

The team taking care of this part is made up of Garret Shook and Rodney Chiu. This is the module that fits on the end of the shell and is separated from the rest of the shell before the flyer is deployed. There are many important parts to this module.

First there are the stabilizing fins. Without any fins, the shell is unstable since the center-of-pressure is in front of the center-of-gravity. Although the fins make the shell stable, they increase the drag, which reduces the overall range. In addition, the fins have to deploy as soon as the shell exits the barrel. Six fins[1] are used in the design as can be seen in figure 9.

1. Shook, Garrett, *Design, Assembly and Test of a Launch and Flight Support and Deployment System for a Gun-Launch Reconnaissance Vehicle*, Massachusetts Institute of Technology, Cambridge, MA, June, 1998

Figure 9: Shell with Six Fins Deployed and Flyer

Then the parachute is an integral part of this back end. The parachute has two tasks. It must slow down the vehicle from a velocity of Mach 2 to 50 m/s. It must also pull the flyer out of the shell. Calculations showed that this required a force of 300N. The parachute was designed with the help of Butler Parachute Systems which designs parachutes for military applications. The final

result was a kevlar parachute attached to the flyer with a swivel joint[1]. Wind tunnel testing of the parachute can be found in figure 10.

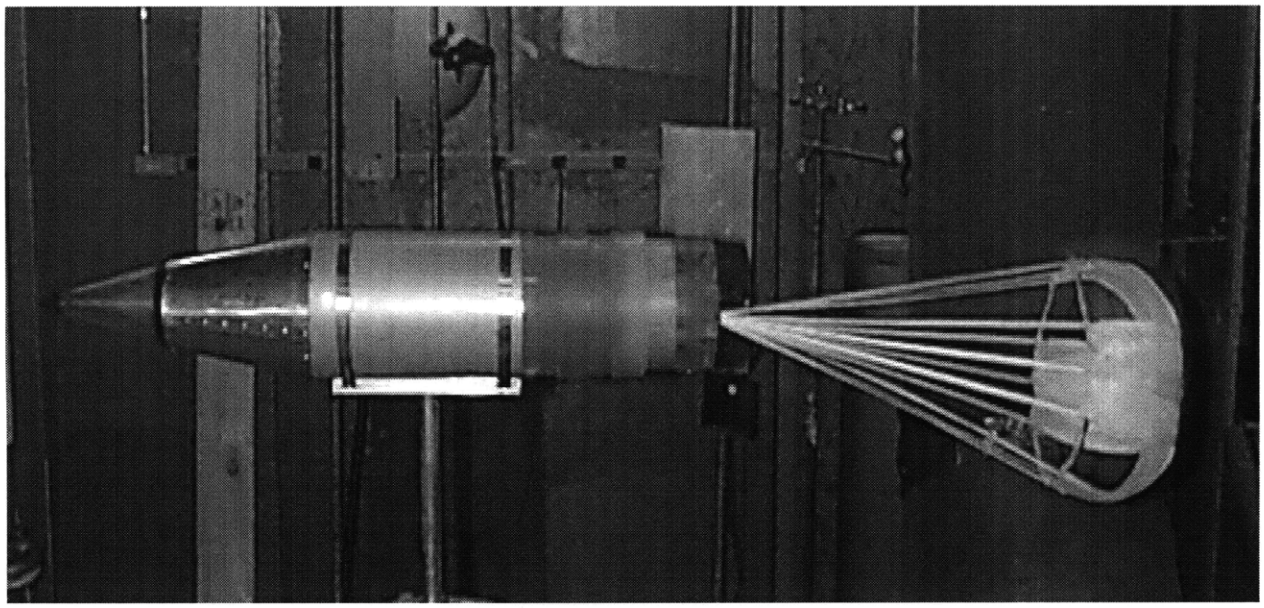

Figure 10: Parachute Deployed in Wind Tunnel

The final task for the back-end was to design the attachment of the back-end to the rest of the shell as well as the separation mechanism.

2.2.2 Tail Module

The tail module includes the tails and most of the electronics. The team taking care of this part comprised Sebastien Katch and myself. This team had the responsibility of designing the deployable tails and packaging most of the avionics in the tail (figure 11). At first two V-tails were chosen as the lone control surfaces for the aircraft. With V-tails, both longitudinal and lateral control could be obtained with only two control surfaces. Later on, the design incorporated a set of two rudders because of lateral instabilities. While the two V-tails are control surfaces (provisions were made so that they can rotate), the rudders are only there for stability purposes and remain fixed during flight. All the rudders and V-tails are designed to deploy as soon as the flyer exits the shell. This is done with a spring loaded pivot. The design of the motion for the V-tails was performed by the author and will be discussed in more detail later on.

---

1. Chiu, Rodney, WASP Deployment Sequence, Massachusetts Institute of Technology, Cambridge, MA, August, 1998

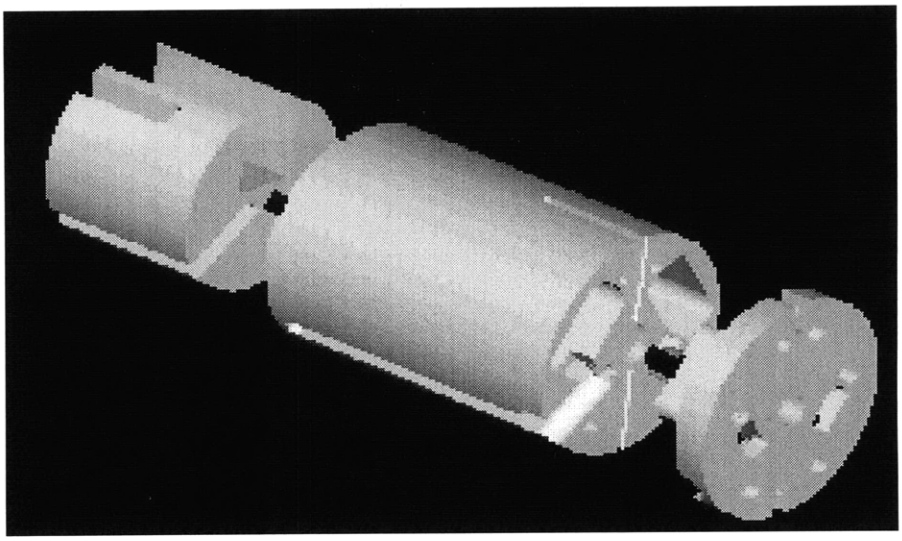

Figure 11: Tail Module

2.2.3 Wing module

The team designing the wings was Stacey Jenkins and Thierry Casiez[1]. To this extent, the whole middle section of the vehicle was reserved for the wings. For the wing design, the major constraint is that they have to be completely enclosed within the five inch shell diameter (figure 12). Two concepts that were initially studied were the foldable wing and the inflatable wing. During the Summer, the foldable wing concept was selected and incorporated into the design.

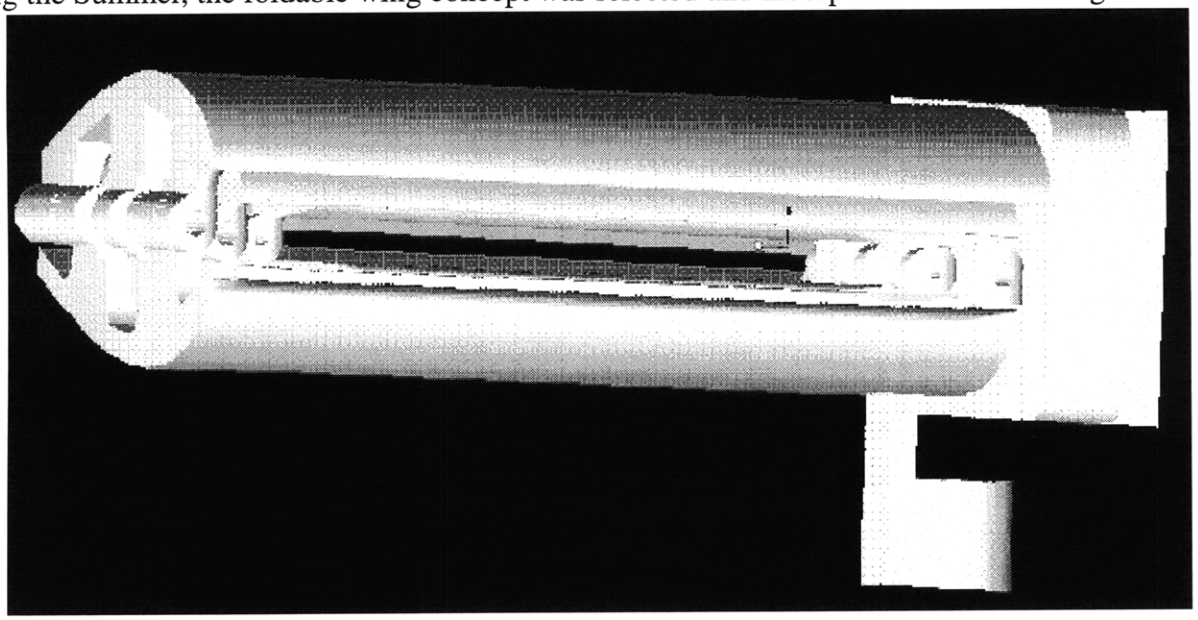

Figure 12: Stowed Wing inside Flyer

1. Casiez, Thierry, *Compact, High-g, High Efficiency Folding Wing for a Cannon-Launched Reconnaissance Vehicle*, Massachusetts Institute of Technology, Cambridge, MA, June, 1998

The wings consist of six airfoil sections attached together by hinges. These spring loaded hinges allow for the whole wing to unfold (figure 13).

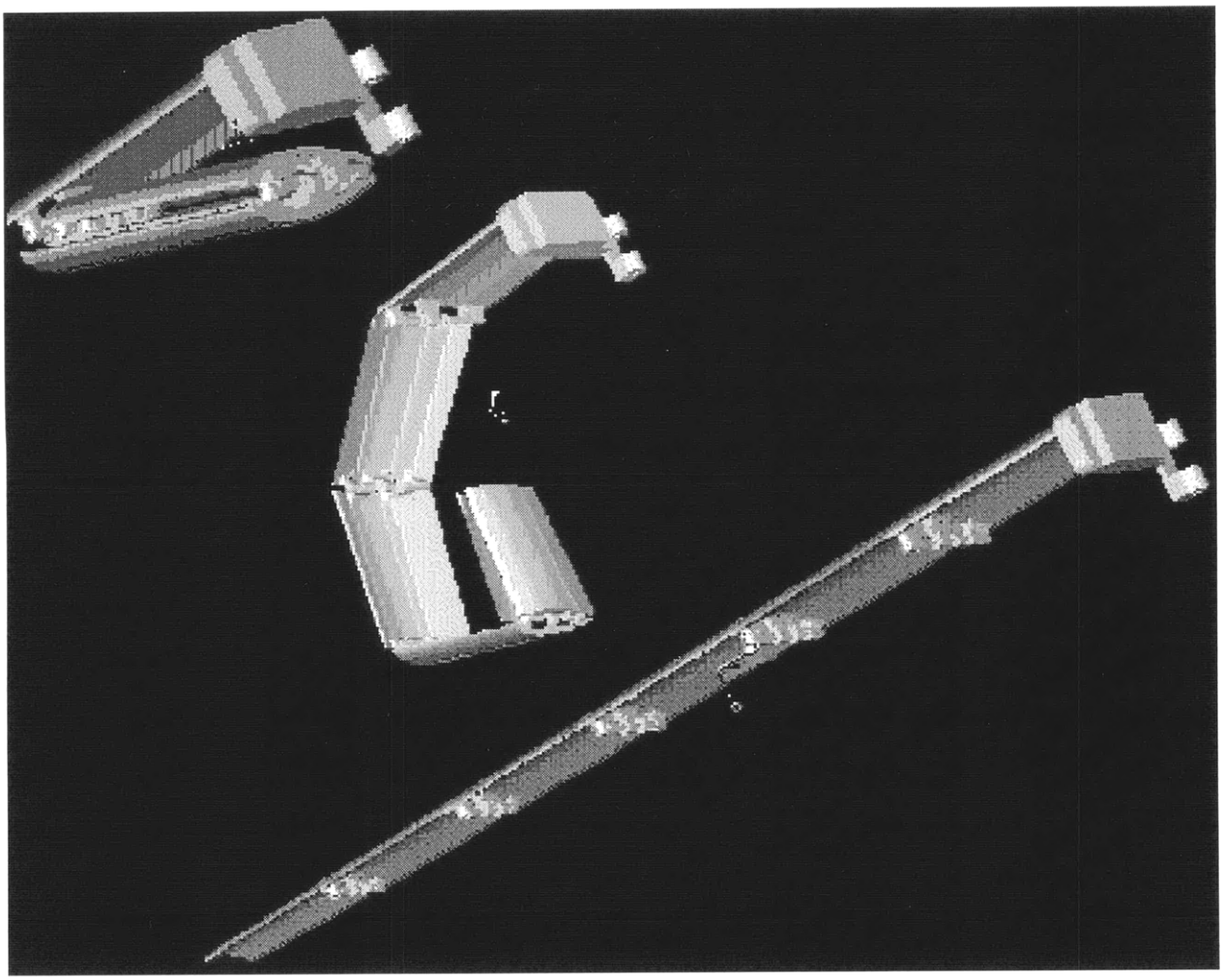

Figure 13: Wing Deployment Sequence

2.2.4 Cone Module

The design of the cone module was performed mostly by Torrey Radcliffe. This cone module includes most of the propulsion unit, which is a gas engine. After testing a few engines in the Picatinny Air Gun, the two-stroke was selected. In addition to incorporating this engine in the cone, a foldable propeller, a staring mechanism, a gas tank, a glow plug and a servo for the carburetor are all needed (figure 14).

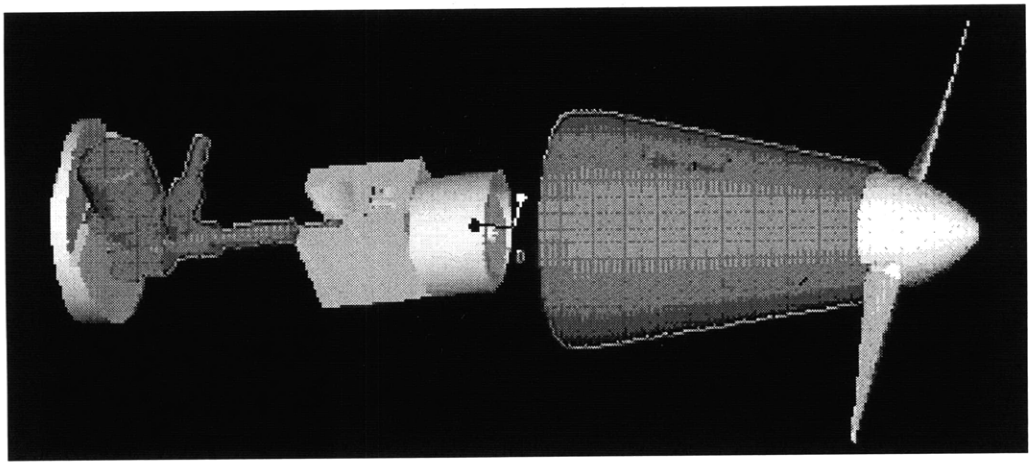

Figure 14: Propulsion Module

2.2.5 Aircraft Stability and Communications

The team taking care of all the software and the aerodynamic control of the aircraft is made up of Tan Trinh and Vladislav Gavrilets[1]. The responsibility of this team was to design the control law to stabilize and steer the aircraft. This included the autopilot capabilities and all the implementation of this control law in software. Since this part of the project dealt with a lot of software issues, it also included the communications aspects. Therefore a ground station had to be designed so that the flyer could communicate with personnel on the ground and relay all the information such as pictures and flyer position (figure 15).

1. Gavrilets, Vladislav, Development of Avionics Systems for Small Unmanned Aircraft, Massachusetts Institute of Technology, Cambridge, MA, June, 1998

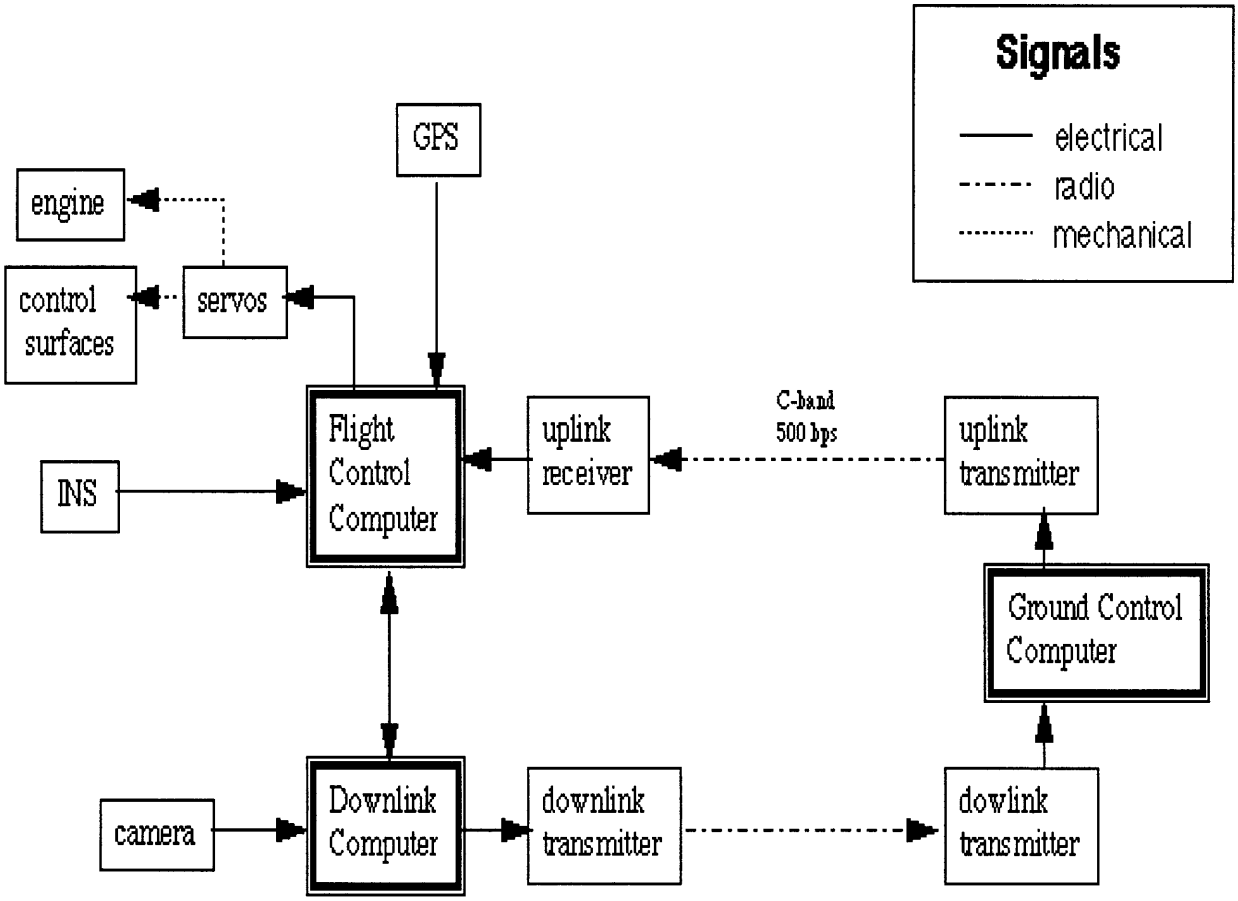

Figure 15: Software Architecture for Operational Vehicle

The FTV was created to be able to prove much of this.

2.2.6 Internal Structure

This part of the project consisted of putting all the different parts together; including designing the connections between the different modules and keeping track of all the interfaces. The combination of all the modules is shown in figure 16[1].

1. Katch, Sebastien, Concept *Development, Mechanical Design, Manufacturing and Experimental Testing for a Canon Launched Reconnaissance Vehicle*, Massachusetts Institute of Technology, Cambridge, MA, June, 1998

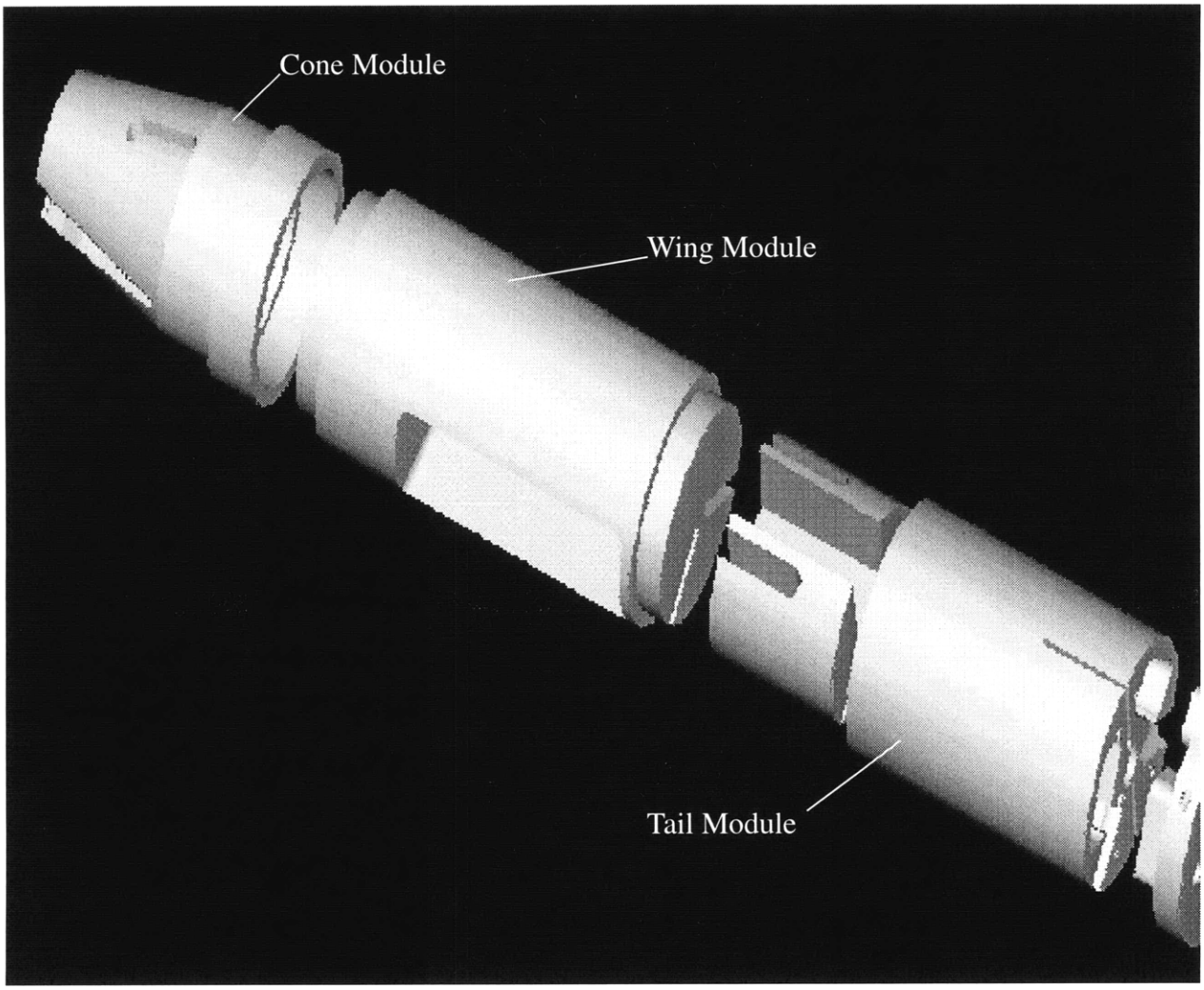

Figure 16: Modular Structure of Flyer

2.3 Overview of Project Work

The author's work was mostly centered on the tail module. This included the design of the tail actuators and design of the power systems. The work on the power system was to make sure that all different components of the flyer got the right current and voltages. For the tail actuators, a servo had to be selected and tested. Then, a set of gears had to be designed to transmit the torque from the servos to the tails.

Another part of the author's work was to look into a backup plan for the propulsion. This included looking for an electric motor and batteries that fit into the design. Finally this combination had to be tested.

As part of these different responsibilities, a few test articles had to be designed and manufactured to test different components in the Picatinny air gun. Some of the individual components tested include batteries, servos, cameras (see figure 17) and an electric motor.

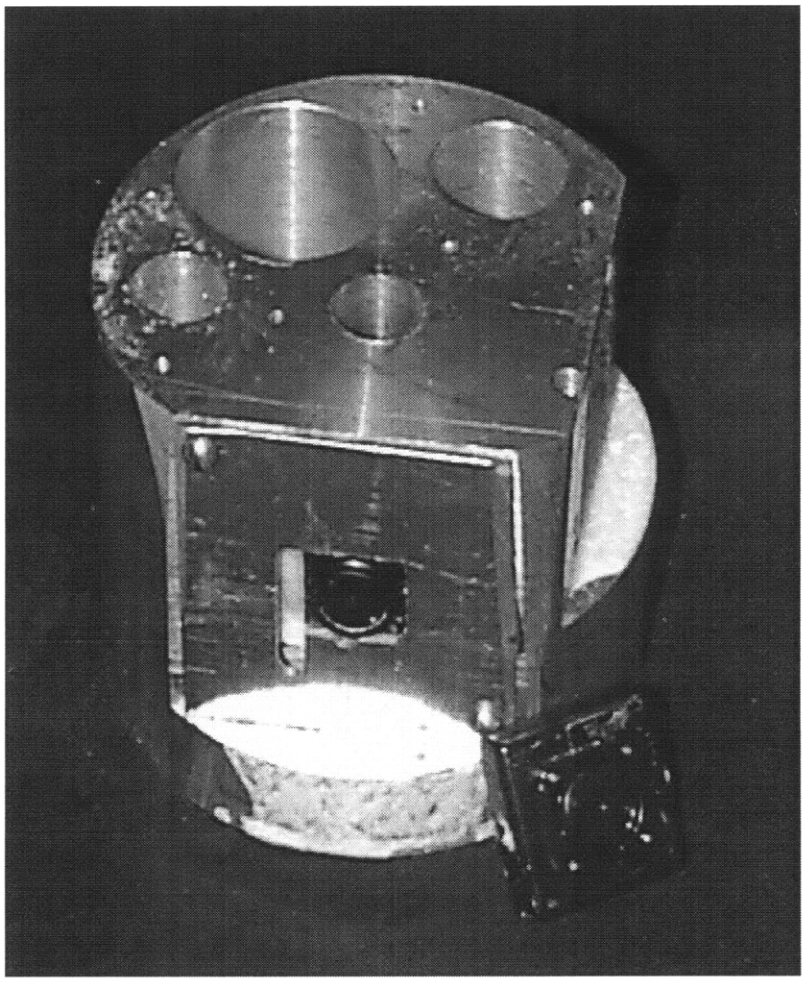

Figure 17: Camera Test Article

Power Systems

The different test vehicles and the final operational vehicle have different components that require electric power for operation. These components, such as the IMU, CPU and explosive bolts, all require power at different voltages and currents. Such a vehicle usually has one or two power sources or batteries. The goal in the design of power systems is then to distribute this electrical power at the right current and voltages to the different components of a vehicle. In addition, the electrical noise coming from the power regulation has to be acceptable to the component. If the electrical noise is too large, the electrical component might not function properly.

This chapter will go over the steps in the design of the power system for the Flight Test Vehicle, the operational vehicle and the High-G Vehicle, which all have different power needs.

3.1 Flight Test Vehicle

In designing the power system for any vehicle, the power requirements of all the components have to be identified. The battery choice will then depend on the power requirements, and the time duration that these components have to be powered.

3.1.1 Power Requirements

Table 1: FTV Power Requirements

Component	I(A)	U(V)	P(W)
GPS Receiver	0.28	5	1.40
GPS Antenna	0.05	15	0.75
IMU	0.23	15	3.50
	0.23	-15	3.50
IMU filters	0.01	15	0.15
	0.01	-15	0.15
CPU	0.98	5	4.90
Ethernet	0.4	5	2.00
Serial Ports	0.4	5	2.00
A/D	0.01	5	0.05
	0.01	12	0.12
	0.01	-12	0.12
Modem	0.2	5	1.00
Servos	0.3	5	1.50
RC receiver	0.014	4.8	0.07
Engine (glow plug)	1.25	1.5	1.88

The Flight Test Vehicle contains most of the avionics included in the final operational vehicle. The different power demands of the components of the FTV are included in table 1.

Of note, the camera's power requirements are not included in this table although it is a part of the FTV. The camera was included in the FTV in the later stages of design. It would be part of the flyer only once all the aerodynamics and automatic piloting have been proven. Therefore, the camera has its own compartment with its own battery.

The RC receiver and the servos are other components that will not be powered by the main battery. The receiver is a mission-critical component of the flyer. If it fails, the system no longer has the option of activating the parachute servo. Such a scenario would probably lead to the destruction of the vehicle since it was not made to survive a landing without a parachute. A backup system was implemented, where, if the CPU no longer receives a command from the receiver, it engages the parachute deployment. In case the main battery fails, the back-up no longer works since both systems are powered from the same source. Hence, it was decided to have a separate battery for the receiver, which would then also power the servos. The receiver and servos have a relatively low power draw, so this secondary battery would always run out of power after the main battery.

Unlike the final operational vehicle, the engine glow plug does not have to be powered by an on-board source. The glow plug has to be turned on for a few seconds before starting the engine. It can then be powered from an outside power source.

Before selecting a battery, the maximum power draw has to be determined. In light of this, the different operating modes of the flyer have to be considered. For the FTV, all of the components might be on during some phase of the flight. The battery therefore has to be able to provide a maximum power equal to the sum of all the individual power requirements. This can be seen in the following table (table 2).

Table 2: Determining the Total Power Requirements

Component	I(A)	U(V)	P(W)
GPS Receiver	0.28	5	1.40
GPS Antenna	0.05	15	0.75
IMU	0.23	15	3.50
	0.23	-15	3.50
IMU filters	0.01	15	0.15
	0.01	-15	0.15
CPU	0.86	5	4.30
Ethernet	0.4	5	2.00
Serial Ports	0.4	5	2.00
4D	0.01	5	0.05
	0.01	12	0.12
	0.01	-12	0.12
Modem	0.2	5	1.00
TOTAL			19.64
		Battery efficiency	x 1.2
		Conversion efficiency	x 1.33
		Total Power Required	**31.34**

In addition to summing up all the power requirements, an allowance must be made for efficiency losses in between the battery output and the component inputs. A 1.2 factor is included for any losses in the batteries, called battery efficiency. Another allowance of 1.33 is included because of losses in the power board. This corresponds to an efficiency of seventy five percent which is a high estimate for typical DC/DC converters.

The significance of these factors is that the battery must provide more power to overcome these losses. These factors are only a first order estimate of the losses and allow for a first iteration in the battery and DC/DC converter selection. Once these two components are selected, the approximations can be re-evaluated and eventually verified.

The next step was to select a battery capable of providing a maximum power of 32W for a period of twenty to thirty minutes. This time includes the setup time to place the flyer on the ultra-light, the time to have the ultra-light take off and release the flyer at the right altitude, and finally the effective flight time. The battery will have to provide power during this whole sequence.

3.1.2 Battery Selection

With all the power requirements for the FTV set, it is now possible to select the right battery.

3.1.2.1 Battery Type Selection

In addition to fulfilling the power requirements of the FTV, the batteries should be low weight and low volume. Since the FTV will be flown on different occasions, it was preferable to have rechargeable batteries to limit costs.

There are different rechargeable batteries that could provide the high discharge rates that are necessary for the FTV. The different options and their implementation can be found in the following table.[1]

Table 3: Rechargeable Batteries Characteristics

	Nickel Cadmium	Nickel Metal Hydr.	Lithium Ion	Lithium Metal
Energy Density (Wh/Vol)	45	55	100	140
Cost ($/Wh)	150	180	225	300

Lithium Metal batteries seem to be the most viable option. These batteries are relatively new. The re-charging mechanism has yet to be refined; only two of these cells can be recharged in series. Since twelve of these cells are needed to make up the battery, the battery would have to be disassembled to have it re-charged. There is also a considerable lead time for the procurement of these batteries.

Nickel Metal Hydride batteries seem to be the next best alternative. They present a 20% higher capacity than the best Nickel Cadmium batteries. They also have been on the market for a longer time. Therefore they do not present some of the inconveniences of the Lithium Metal bat-

1. Pnina, Dan, *How to Choose a Rechargeable Battery*

teries. It was later found out that there are doubts as to whether these batteries can withstand engine vibrations. There were instances in the Aircraft Radio Control market, where some nickel hydride batteries would explode due to engine vibrations. The batteries would then expunge gases at 300^{o}C.

These results were not experimentally verified, but for risk management, it was not worth having this happen during a test flight. The currents required for the given application (about 2A) are pushing the envelope of these batteries since they usually only give about 0.5 C or 0.65A.

The Nickel Cadmium batteries ended up being the best option since they can provide high currents and have been used in the RC Aircraft industry for a while.

Having picked a battery type, the cell size must now be selected. From an analysis on the power density done for the electric motor, the AA size cells are the most efficient size when it comes to power per unit volume. This analysis can be found in detail in chapter five. The KR 1100 was therefore selected as it is a AA cell with a 1.1 A.h capacity (slightly higher than that of the N-3US).

3.1.2.2 Battery Quantity Calculation

The main specifications usually available for a battery are its capacity and voltage. The capacity is the current that the battery can provide for one hour. For the calculations, the power that can be provided by each battery is given by:

$$Power = DischargeRate \times Capacity \times Voltage$$

The discharge rate is given as a factor of the capacity. There are empirical curves that give the capacity as a function of discharge rate. Using these curves for the KR 1100, the following results are obtained.

Table 4: Battery Lifetime vs. Number of Batteries

Number of Cells	Discharge Rate (C)	Maximum Power (W)	Time (min) @ max P
120	0.2	32.7	300
24	1	31.7	54
6	4	32.2	12
3	8	30.9	5.25

For different discharge rates, the number of cells necessary to obtain 32 W is computed. From here, the lifetime of the battery can be obtained from the capacity. Using this table, the run time at thirty-two watts can be plotted vs. the number of batteries used (figure 18).

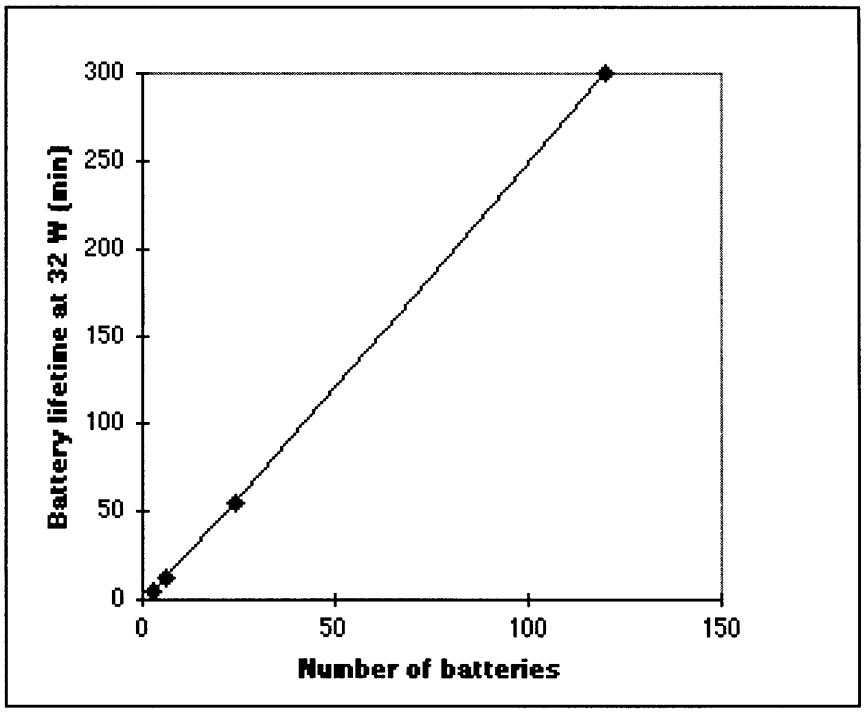

Figure 18: Battery Lifetime

It can be seen that the relationship is nearly linear. The effects of lower voltage and reduced capacity at the higher discharge rates are not noticeable. Extrapolating between the extreme val-

ues of the curve, 11.9 or twelve batteries are necessary to run at 32 W for thirty minutes. Consequently, a battery pack of twelve batteries was used for the FTV. A safety margin is not necessary here. 32 W represents the maximum power drawn from the batteries, meaning that less power will be drawn for most of the time.

The cells were formed into a welded battery pack by the same company the cells were ordered from (figure 19). After assembly, the final battery pack has a voltage of 14.4 V.

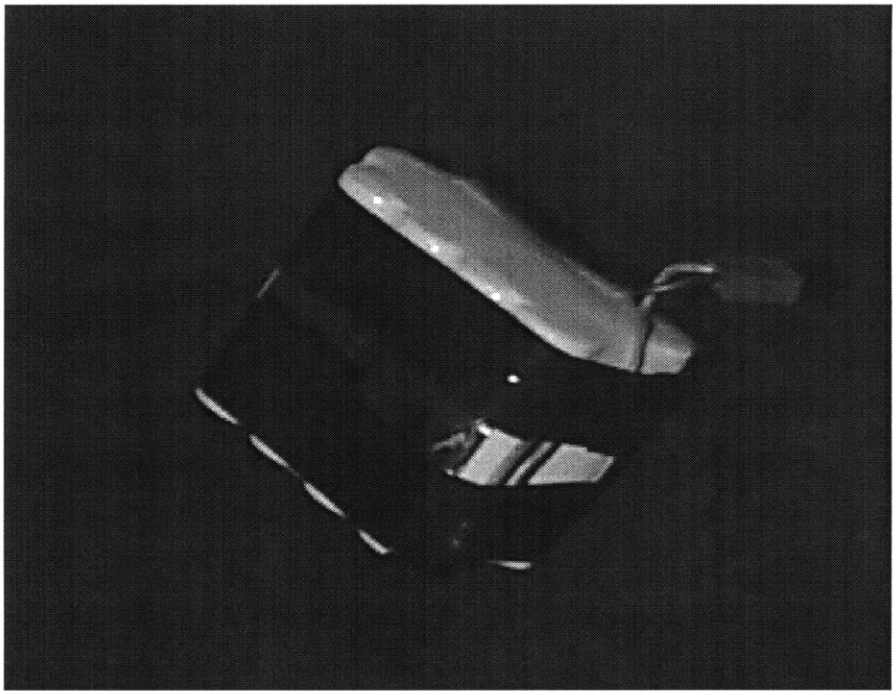

Figure 19: Picture of FTV Battery

3.1.3 Power Module Design

The design of the power module is divided in two. First the power board is designed. Then, the power board and battery are incorporated into the rest of the FTV design.

For power distribution, five different voltages are needed: 5V, +12V, +15V, -12V, -15V. Some components of the FTV such as the CPU, ethernet and A/D converters need good power regulation. They can not accept wide variations in voltage and noise. On the other hand components such as the IMU and GPS units are more robust and can accept a greater range of voltages and noise in the input signal.

For the sensitive avionics, there exists a PC104 card which acts as a DC/DC converter giving voltages of 5V and +/-12V. This card is usually paired with the CPU used and was selected to power the CPU, ethernet, serial ports and analog to digital converters. For the PC 104, the input range is very wide (eight to thirty volts DC), and does not require any voltage regulation at its input. The card can be considered a black box with an input from the battery and outputs to the different components.

The other components require 5V and +/-15V. These voltages are obtained with a DC/DC converter and no filtering of the output. A commercially produced triple output DC/DC converter which can give up to 20W of output power was selected. For the DC/DC converter, the input voltage range was 9-18 V therefore placing the 14.4V of the battery pack close to the middle of the acceptable range.

The layout of the power board with all the connections is represented in figure 20.

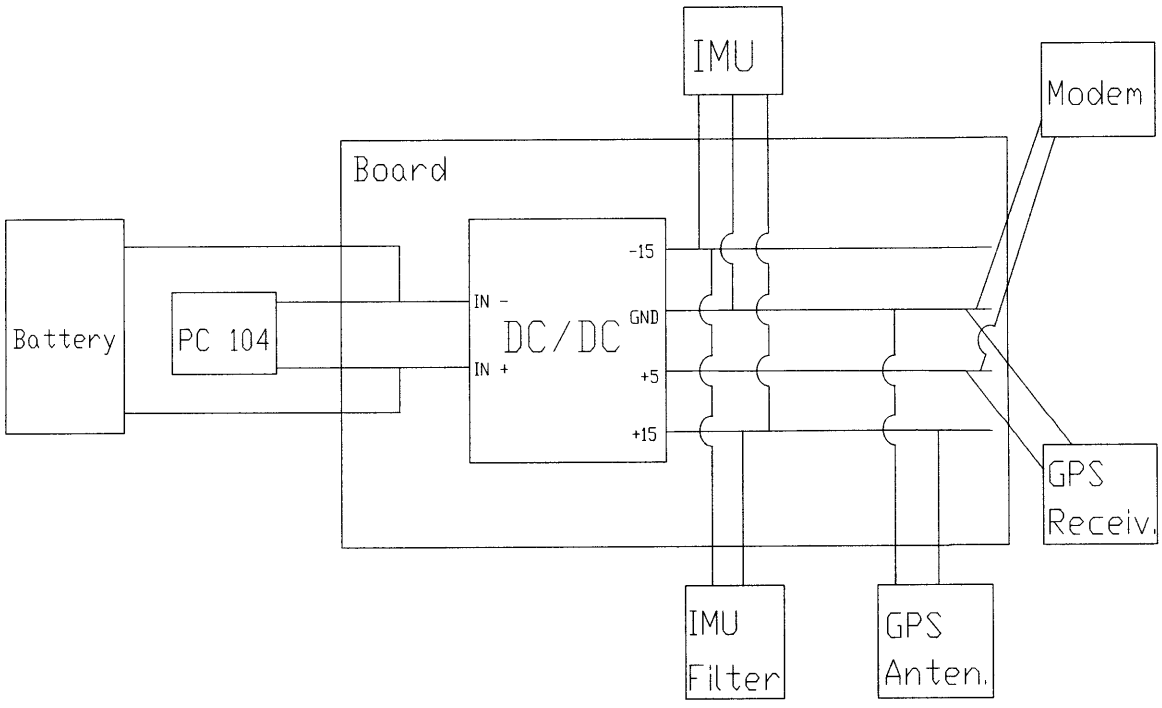

Figure 20: FTV Power Board Circuit Diagram

The DC/DC converter was soldered along with connectors onto the board itself. Use of connectors was advantageous since all of the components could be plugged and unplugged during assembly and testing.

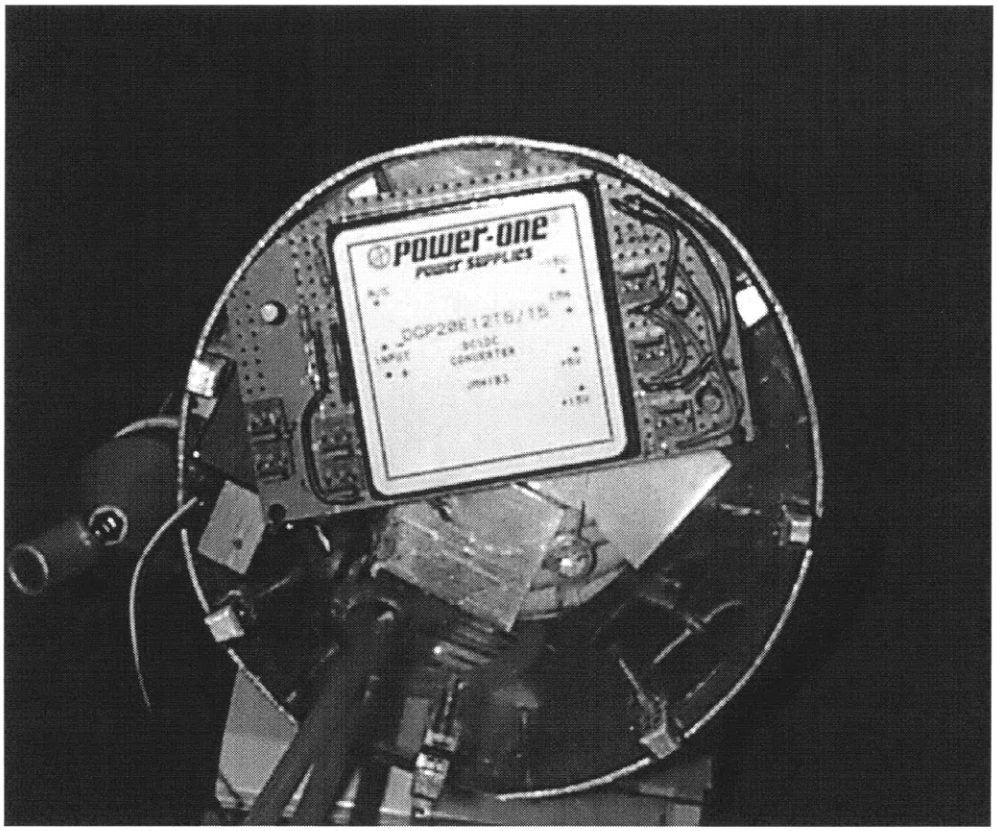

Figure 21: Power Board inside FTV

The power board was screwed on to the backside of the engine mount, as seen in the above picture (figure 21). With the use of foam, the battery is fixed into place next to the power board.

3.2 High-g Vehicle

3.2.1 Power Requirements

The power requirements for the high-g vehicle are much different since the high-g vehicle does not contain any of the avionics. The high-g vehicle needs power primarily to engage different mechanisms in the deployment sequence. These are mostly explosives that require high power for very short periods of time.

Table 5: High-g Vehicle Power Requirements

Component	Voltage (V)	Current (A)	Power (W)	Time Duration (s)	Resistance (ohms)
Explosive Bolt	5	5	25	0.01	1
Shape Charge	5	5	25	0.01	
Glow Plug	1.25	2.5	3.125	15	
Piston Actuator	1.6	0.15	0.24	0.01	4-9.5
Gas Generators	5	5	25	0.01	

3.2.2 Power Source Selection

The power requirements for the high-g vehicle can be achieved in multiple ways. A battery could be used to deliver short pulses of 25W. But as with the operational vehicle, there is the problem of finding a battery giving off such high currents. A battery of the size of the operational vehicle's battery would then have to be used.

Another option is to use capacitors. Capacitors can give off the high discharge pulses required. There are two ways to use the capacitors. They can be charged up with a battery during the flight. This has the advantage of only requiring one capacitor. Another option would be to pre-charge the capacitors before the launch. This requires as many capacitors as there are discharges, five for the high-g vehicle. A disadvantage of pre-charging a capacitor is that the shell with the pre-charged capacitors would have to be fired in a timely fashion. The capacitors discharge with time and would lose much of their charge after a few months. This is not a big issue for the high-g vehicle, since the capacitors would be put into the shell and pre-charged only a few days before the launch. The advantage of the pre-charged capacitors, is that an extra electronic circuit, to obtain the right charge-discharge sequence from the capacitor, is not required. Another advantage is that pre-charged capacitors can be charged to higher voltages than capacitors charged by the on board bat-

tery. This means that smaller capacitors could be used since they contain as much energy as larger capacitors charged by the on-board battery.

3.2.3 Power Board Design

The design of the power board for the high-g vehicle is as follows (figure 22).

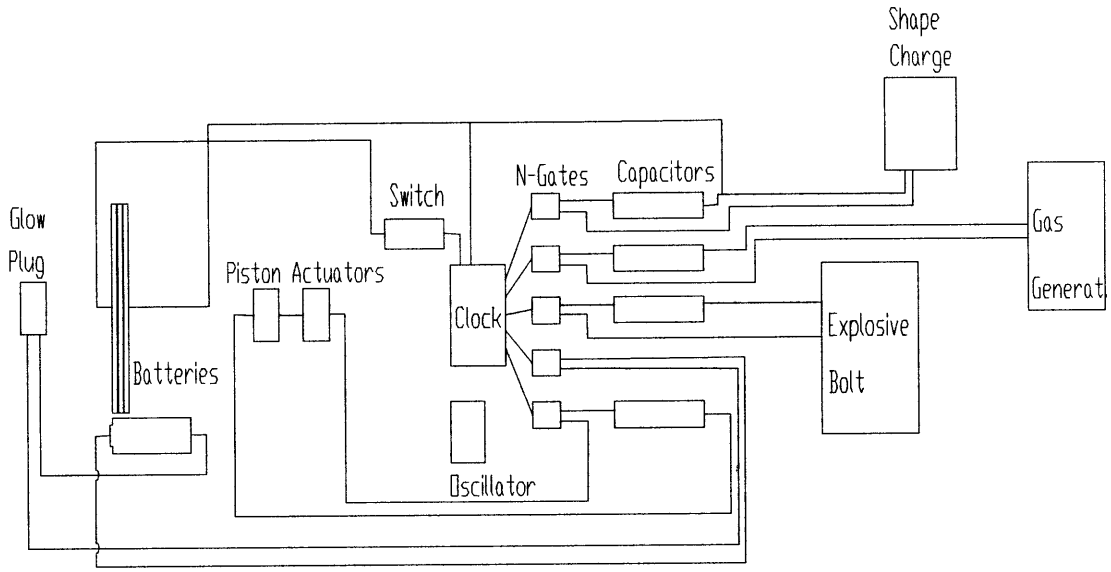

Figure 22: High-g Vehicle Power Board Design

The five components to be powered are shown. The sequence of events for the activation of the different components is as follows. A high-g switch engages the circuit when the shell is fired. This switch closes when it senses a g-loading above 400 g's. The closing of this switch starts a digital timer. When the clock reaches the deployment time of a certain component, it sends a small current to the N-Gate. The role of the N-gate is to act as a switch when it receives a small current from the third channel (the clock). This closes the circuit and discharges the capacitor through the component.

The design of this power board is only preliminary since the plan for the high-g vehicle changed from being a deployed flyer to a canister test in the real gun. This canister test no longer

required any activation from a timer so this power board is not required for the first high-g test at Dahlgren.

3.3 Operational Vehicle

The power system for the operational vehicle will be very similar to that of the FTV. The main difference is that the operational vehicle's power system has to be g-hardened. Also, the operational vehicle's components are also slightly different than the FTV's.

3.3.1 Power Requirements

The power requirements for the operational vehicle can be found in table 5.

Table 6: Operational Vehicle Power Requirements

Component	I(A)	U(V)	P(W)
GPS Receiver	0.64	5	3.20
CPU	0.053	12	0.64
+ other Draper	0.046	-12	0.55
components	0.6	5	3.00
IMU	0.024	12	0.29
	0.024	-12	0.29
	0.48	5	2.40
Servos	0.2	4.8	0.96
Engine (glow plug)	1.25	1.5	1.88
UHF Transmitter	0.3	12	3.60
Camera	0.1	12	1.20
Modem	0.8	5	4.00

The components of the operational vehicle are different than the ones for the FTV, hence they require different amounts of power. Of note is the addition of a glow plug for the engine since the engine has to be started in flight and cannot be started externally on the ground, as in the FTV. Also, some components require significantly more power because of the different functionality of the FTV. For example the power requirement of the modem is four times greater for the operational vehicle since that vehicle will have to communicate over much greater distances. Similarly, the power requirements of the servos are greater for the operational vehicle since it flies faster, resulting in higher dynamic pressure loads on the control effectors.

As will be seen in the following section, there was a need to reduce the maximum power drawn from the electronics. This maximum power had to be reduced from just being the sum of all the powers. The glow plug power could be removed from the total power requirements since it did not have to be on with all the electronics. The glow plug would be turned on before all the electronics are started. It therefore does not figure into the total maximum requirements.

The different operating conditions were identified to see if the total power requirements could further be reduced. A scenario was envisioned where the UHF transmitter and camera are turned on intermittently. The camera would take a picture and then turn off. At this point the transmitter is turned on and sends the data from the camera. In this sequence, the camera and transmitter are never turned on together. Therefore the camera power is removed from the maximum power requirement.

With these considerations, the following table is obtained to determine the total power requirements. Again there is a 1.2 allowance for battery losses, and a 1.2 allowance for conversion losses. It should be noted that the conversion loss for the operational vehicle is lower than for the FTV, which had a factor of 1.33. It was assumed that the operational vehicle will have a more expensive, higher quality DC/DC converter. These converters usually have efficiencies in the 80-85% range (corresponding to a 1.2 factor).

Table 7: Operational Vehicle Maximum Power Required

Component	I(A)	U(V)	P(W)
GPS Receiver	0.64	5	3.20
CPU	0.053	12	0.64
+ other Draper	0.046	-12	0.55
components	0.6	5	3.00
IMU	0.024	12	0.29
	0.024	-12	0.29
	0.48	5	2.40
Servos	0.2	5	1.00
UHF Transmitter	0.3	12	3.60
Modem	0.8	5	4.00
TOTAL			18.96
		Battery efficiency	x 1.2
		Conversion efficiency	x 1.2
		Total Power Required	**27.31**

With these adjustments, the maximum power required from the operational vehicle battery is about 27.3W. The goal was for the battery to provide this much power for twenty minutes of flight time.

3.3.2 Battery Selection

For the operational vehicle, there exists some batteries on the market capable of withstanding 15,000 g's. Eagle Picher has a division dealing only with military batteries. And according to Carlo Venditi at Draper, their batteries were the best on the market for this application. An attempt was made to contact other possible manufacturers of high-g batteries without any success. Eagle Picher basically markets two types of batteries that are relevant to the operational vehicle. There are primary batteries which are Lithium Thionyl Chloride in this case. These batteries offer the high rate of discharge necessary for this application. The different types of cells and batteries that are relevant to this project are included in the following table (table 7).

Table 8: Eagle Picher High-g Batteries

Part #	Voltage (V)	Capacity (Ah)	Peak Discharge (A)	Volume (cm^3)	g loading ($9.8 m/s^2$)	Volume to deliver 27.3W peak (cm^3)	Volume to deliver 27.3W for 20 min
LTC-511	3.65	0.375	0.6	5.74	15,900	74.6	40.2
MAP-9217	3.65	0.0011	0.01	0.1212	23,000	90.7	274.8
MAP-9233	36.5	0.375	0.6	102	15,900	204.0	102.0
GAP-9146	14.8	1.1	0.025	83.4	18,000	6171.6	83.4
GAP-9218	3.65	0.001	0.01	0.123	23,000	92.0	306.8
GAP-9246	18	0.00146	0.1	1.93	17,800	30.9	669.7
GAP-9254	11 22	0.294 0.073	6 0.07	91.68	30,000	 91.7	 183.4

Two different numbers can be derived from the information on the batteries. One of them is the battery volume required to provide the 27.3 W of peak power. The other important value is the battery volume required to provide maximum power for twenty minutes. This second number depends on the total energy of the battery and does not depend on the maximum power the battery can discharge. The battery will have to satisfy the two requirements, therefore it will have to occupy the larger of the two volumes. The LTC-511 and the MAP-9233 are the two best options.The problem with the LTC-511 is that they are cells, and will take up much more space when many of them are put together. The MAP-9233 combines ten LTC-511s, but takes up much

more space than ten LTC-511s. Therefore the best solution using these batteries was to use two MAP-9233s.

Thermal batteries are another existing high-g battery type. The main advantage over primary batteries is that they have unlimited lives. The down side is that their run time is very short. They can give very high rates of current for about ten minutes before running out. An analysis on the thermal batteries is included in the electric motor chapter. This will show that the thermal batteries do not provide power for a long enough time, and that they have not been tested to the g-levels that are required.

Finally the last option is to use off-the-shelf batteries that were tested to see if they could withstand the g-loads. Nickel Cadmium and Nickel Metal Hydride were the best choice because they provide the highest current. Nickel Cadmium can give off many times their capacities. One of the Nickel Cadmium and a Nickel Metal Hydride batteries were tested in the Picatiny Air Gun at loads of 15000 g's. After a first test the Nickel Cadmium battery, a Sanyo 1300 KR, did not survive. More on this test can be found in chapter 5. The Nickel Metal Hydride survived the first launch. It gave the same voltage reading after the test as it did before the test. A second test at a little over 15000 g's was inconclusive. The battery was not checked immediately following the test. When the battery was withdrawn from the canister three days later, the battery had no voltage reading. A third test of this battery failed. This meant that the Nickel Metal Hydride could not survive the acceleration with high reliability. Hence it could not be included in the design.

It was also found during the late stages of the design that the typical Duracell 9V battery had survived gun launches and was being used on other similar projects. These nine volt cells could provide enough power and flight time while reducing the space required. Four of these batteries were tested in the final Dahlgren test.

3.3.3 Power Board Design

Since the PC-104 card was not g-hardened, the power board of the operational vehicle would have to distribute the power to the very sensitive items such as the CPU. Therefore this power board also required some additional filtering of the power after the DC/DC converter. To do this, the noise tolerances of all the components would have to be experimentally determined. Since

most of the high-g electronics were not available to the team, this could not be done with rigor. Also, the design of a high-g power board for the operational required much more knowledge and experience than the author had. Therefore the final design of the power board was deferred to Draper, once the MIT part of the project was complete, and all the components were available.

Tail Actuators

The flyer requires actuators to rotate the two V-tails. To be able to control the aircraft, the tails have to be able to rotate through some angle at a certain rate. First, a servo-motor had to be selected to be able to perform this task.With the servo-motor selected, it was then possible to connect the servo to the tail with a worm gear mechanism.

4.1 Servo-motor Selection

4.1.1 Servo Requirements

The technical requirements for the servo-motors are as follows:

- **static torque = 0.0916N.m**

This comes from the aerodynamic data and the way the tails were designed. The axis along the pivot, about which the tail would rotate, does not pass through the aerodynamic center of the tail. Therefore, under static conditions, the tail will exert a moment on the servo. The servo has to be able to provide enough torque to counterbalance this moment (figure 23).

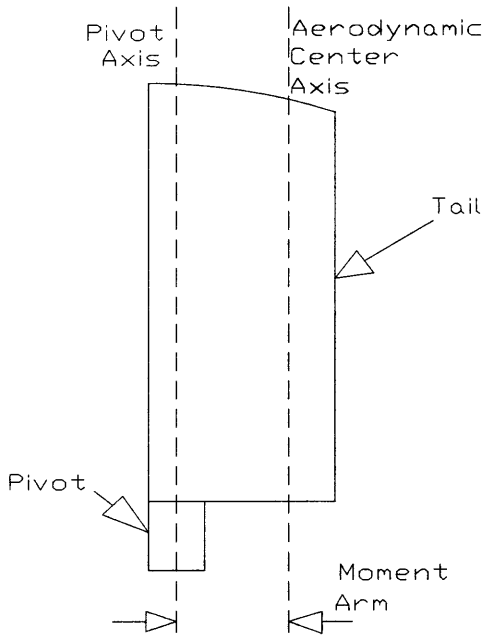

Figure 23: Illustration of Moment Arm

This value of 0.0916 N.m comes from multiplying the moment arm by the maximum lift force on the tail (at the maximum angle of attack) at a cruise speed of forty seven meters per second. Since work on the servos was started at a preliminary stage of the design, this is actually an over-estimation. Indeed, the final cruise velocity was around 39 m/s. Since lift is proportional to velocity squared, the required static torque is then 0.0631 N.m for the final cruise speed. The tails will have to rotate which means that a larger torque is required for the dynamic case. Any extra torque determines how fast the tail will move from one position to another. Since dynamic calculations are much more complex and no requirements on servo response times were available, it was decided to find a servo supplying a torque greater than the static torque required.

- **range of motion = +/- 8^o**

This comes from the controls' team and the aerodynamic characteristics of the airfoil used for the tail. The tail stalls at some angle-of-attack. After the stall point, the tails no longer generate any extra lift and therefore control capability can degrade. To be sure that the design would still work if this requirement changed, it was decided to design a servo with a range of motion of +/-10^o.

- **space constraints**

At the time the servo design was started, the tails and their location were already designed. Hence, the servos had to be positioned around that. A pivot allowing for the tail to deploy had to be placed between the servo and the tail. Because of geometry, the servo rotation axis could not be placed along the same axis as the pivot. To make the servo fit in the tail module, the rotation axis of the servo had to be orthogonal to the axis of the pivot. Hence, a gearing mechanism is necessary to transmit torque between orthogonal axes.

4.1.2 Servo Testing

Servos are made up of a motor and gearing system to allow for the motion, and an electronic card to allow for the position control of the motor. Coming up with a g-hardened motor-gear-electronics combination was beyond the scope of this project. Upon disassembly of an off-the-shelf, commercially produced servo usually used for R/C aircraft, it was apparent that it might be possi-

ble to g-harden the servo. Draper uses epoxy to g-harden their electronics. It is accepted that if none of the electronics have overheated during the placement of the epoxy, then an electronic card will survive the gun launch. The way the servo was made, this epoxy could easily be inserted to immobilize all non-moving parts. It was decided to test a few of these commercial servos in the Picatinny Air Gun after g-hardening with epoxy. Three very different types of servos that could provide more than enough torque were selected, not knowing which servo characteristics would survive better under a gun launch.

Table 9: Servos Tested in Air Gun

Type	Main Characteristics	Max Torque (N.m)	Dimensions (inches)	Cost ($)
S3101	Micro precision servo	0.2118	0.5 x 1.06 x 1.12	28.99
S9101	Coreless, ball bearing servo	0.2944	0.77 x 1.52 x 1.36	59.99
S9203	Coreless, steel gear servo	0.5394	0.79 x 1.59 x 1.48	99.99

A micro-servo was selected because of its small size, which means it could more easily be integrated in the tail. The S9101 represents the typical servo used on most R/C aircraft. It has a coreless motor which might better survive the g-loading. The last servo was selected because of its steel gears. It is a high-performance servo since it gives considerably more torque than the regular servos. Since the gears are made out of steel, the servo might survive the g-loading better. On the other hand, the gears are much heavier which means they might not withstand their own weight.

A test article was designed so that all three servos could be tested at once. The servos were put in the same position as they would eventually be inside the flyer: with the rotation axis parallel to the g-loading axis, and with the shaft pointing out the end of the test article. A test article was machined out of aluminum with three cavities to place the servos. Cavities were machined so that the servo would fit as closely as possible into the cavity. Perfect rectangular cavities can not be machined with traditional machine tools. The minimum radius of a square cavity is the radius of the mill tool used. This leaves a gap along each side of the cavity. Using geometry, the minimum gap size can be calculated as a function of the tool radius. The corresponding calculations can be found in Appendix A.

Each cavity was closed with thin aluminum plates screwed on to the aluminum block. The plates keeping the servos inside the cavities did not need to be very strong since there is no set-back acceleration in the air gun. Holes were placed at the bottom of each cavity so that the servo shaft could stick out through the end of the test article. This allowed for the opportunity to check whether each servo was still working in between tests. The depth of these holes was made so that the shaft could then rest on the canister itself. If the shaft was not left supported like this, then the servo shaft would probably just rip out of the servo during the firing. For the testing, the epoxy was put inside the servos as well as inside the cavities of the test article (outside the servos).

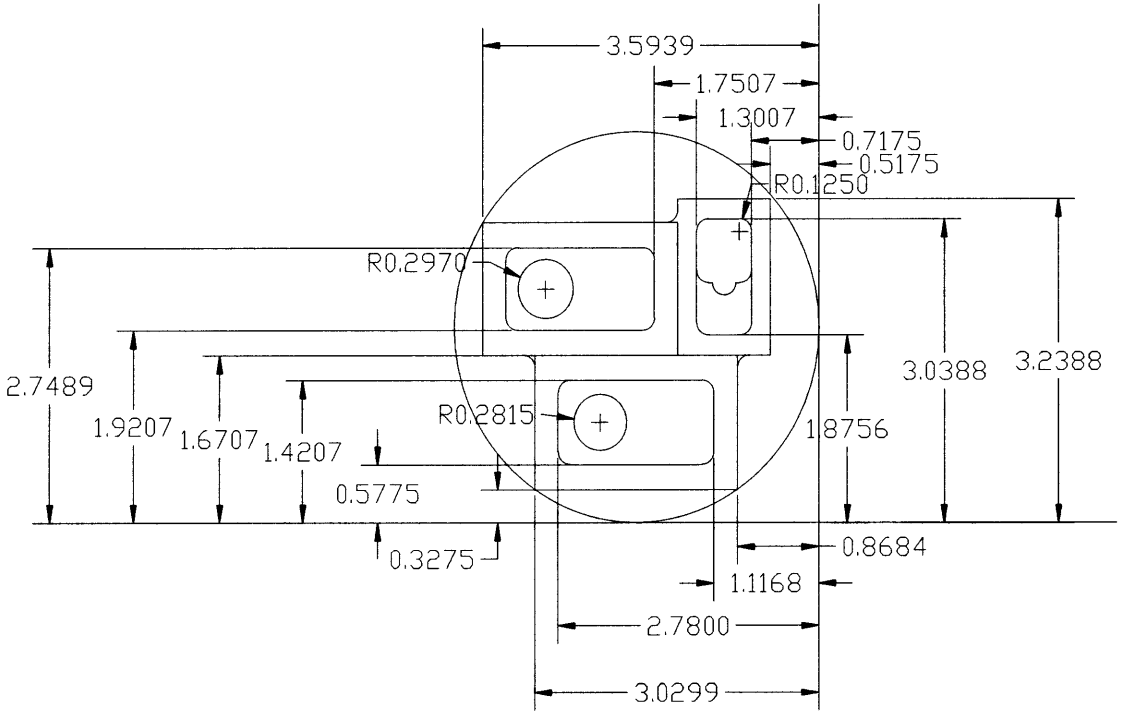

Figure 24: CAD Drawing of Test Article for Servos (dimensions in inches)

The gears of the micro-servo were broken during the g-hardening phase, therefore it was not verified if that servo could survive the g-loading. But it was later verified that the motor was still working. Even though it was not confirmed that the servo could survive the gun launch, it was still incorporated in the engine module as the servo for the carburetor. Its survivability was eventually tested in the real gun canister test at Dahlgren. The 2nd servo survived all four gun launches at:

5,000, 10,000, 15,000 and 20,000 g's. The steel gear servo was not g-hardened satisfactorily. Because of the way it was manufactured, there was no access to the inside of this servo so that epoxy could be inserted. Of note, the electronics card was not g-hardened. This servo did not survive the 15,000 g firing probably because of this. The failure of this servo reinforces the idea that using epoxy helps in g-hardening a servo. Indeed, the servo, which was not properly g-hardened, failed. Since the S9201 is the only servo to have withstood the accelerations of the four tests, it was chosen as the servo to be used for the tail actuators. This made us confident that it could also survive a single acceleration in the real gun which has a longer pulse duration.

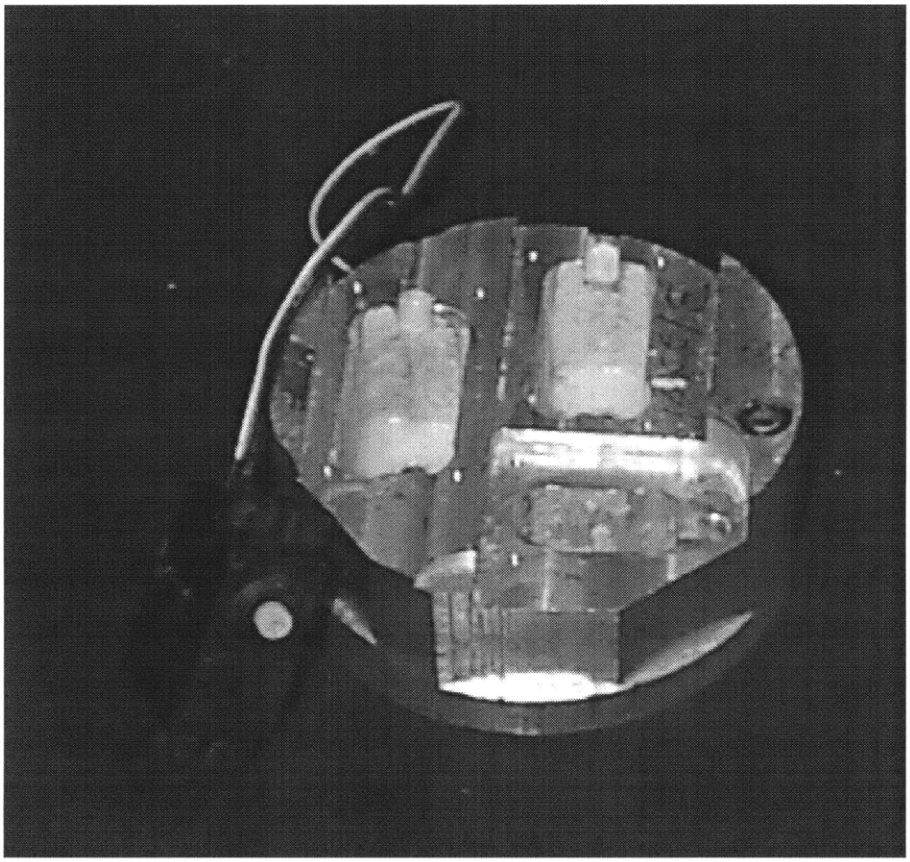

Figure 25: Test Article for Servos.

Type	Test Results	Decision
S3101	Servo damaged prior to test, motor survived	used as engine servo
S9101	Servo survived all tests	used as tail servo
S9203	Failed test at 15,000 g's	not used

Table 10: Testing Results for Servos

4.2 Gear Selection

Since the axis of the servo and the pivot for the tail were orthogonal to each other, a worm gear had to be designed.The functionality of the worm gear was not only to increase the torque output of the servo but also to transmit the torque between orthogonal axes.

4.2.1 Gear Specifications.

With the servo selected, there was a general idea of where the servo would be placed in the tail module. The axis of the servo had to be on a line perpendicular to the pivot so that a worm gear could then be placed in between.

From the requirement that tail motion had to be +/-10^{o}, a general idea of what the gear ratio should be was obtained. By mechanically moving the shaft of the servo, it was determined that the Futaba servo used had a range of motion of 180^{o}, or +/- 90^{o}. Beyond that, there are mechanical stops that prevent the shaft from rotating. To be on the safe side, the maximum rotation of the servo was taken to be +/- 50^{o} to obtain the +/- 10^{o} of rotation of the tail.

4.2.2 Gear Calculations

To decide which gears were eventually going to be used, calculations were performed to get a first approximation of the characteristics needed from the gears. The most important requirement was that the distance between the center of the pivot and the center of the servo shaft had to be around 2 cm. This constraint had to equal the sum of the radii of the worm and worm gear. The worm radius was chosen to be 0.5 cm, and the worm gear radius to be 1.5 cm. From geometry, the axial displacement along the worm is related to the tangent displacement along the gear by the tangent of the angle of the teeth on the worm:

$$l_g = l_w \times \tan\lambda$$

A 10^{o} displacement of the tail or gear is desirable, therefore l =1.5 x 10 / 360 x 2pi= 0.261 cm. This was approximated to 0.3 cm to be sure there was enough worm displacement. The worm gear

rotates by 120° for a full revolution of the worm. Therefore the lead L is 12 x 0.3 = 3.6 cm. For a full revolution of the worm, the tangent displacement along the gear will be 3.6 cm. From the preceeding equation, the pitch angle is given by:

$$\lambda = \text{atan}\left(\frac{L}{\Pi \times d_w}\right) = \text{atan}\left(\frac{3.6}{\Pi \times 1}\right) = 48.9^o$$

The torque required from the servo is given by:

$$T_{servo} = T_{tail} \times \tan\lambda \times \left(\frac{r_w}{r_g}\right) = 0.0916 \times \tan 48.9^o \times \frac{0.5}{1.5} = 0.035N$$

Therefore numbers were obtained for the characteristics of the gearing combination that were necessary:

- worm radius = 0.5 cm
- gear radius = 1.5 cm
- lead = 3.6 cm
- pitch angle = 48.9°

With such a gearing mechanism, about 8.4 times more torque than statically necessary was obtained.

4.2.3 Gear Selection

It was planed to design and machine the worm gears according to these exact specifications. This proved to be too difficult and unnecessary since worm gears have complex geometries to ensure that the worm and worm gear teeth match well. Then the worm gears produced by different manufacturers were identified to see if they could be incorporated into the design. The preceeding calculations were made in the reverse order to see if the required tail motion could still be achieved. Three sets of gears that could be incorporated into the design are included in the following table.

Table 11: Possible Gearing Combinations

Gear Combination	worm pitch radius (cm)	worm gear pitch diam (cm)	servo rotation to get a 10° rotation of tail	Servo torque required (N.m)
W16S-4F + W16B35-F20	0.79375	1.5875	50	0.0184
1C5-Z24 + 1B6-Z24024	0.635	1.27	60	0.0153
WAS-8F + WAB88-F20	0.8	1.5	50	0.0184

The third entry from the preceeding table was selected as the final worm-worm gear combination. It was selected because the sum of the two radii was closer to the initial requirement of two centimeters. It also did not require such a large angular range of motion from the servos. The specifications of the selected mechanism do not exactly match the requirements that were derived. The biggest change is that the distance from the pivot axis to the servo axis had to be increased from 2 cm to 2.3 cm.

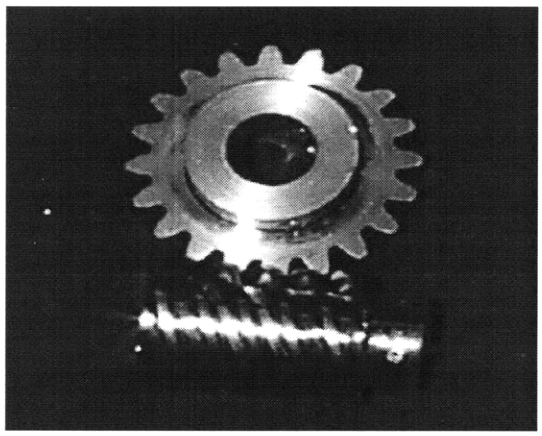

Figure 26: Worm-Worm Gear Combination Selected

4.3 Tail and Gear Integration

Next, the task was to incorporate the tail, pivot, gearing system and servo into the tail module. First, the right position to place the servo and gears in the tail module had to be found. The only degree of freedom available was changing the angle of the servo with respect to the horizontal. The angle of the tail axis was already set by the angle of the V-tails. And, the position of the servo's shaft is also set. It is constrained by the length of the pivot and by the sum of the radii of

the two gears. Therefore the servo was rotated and the final position picked with the wall thickness maximized. This can be seen in the following figure.

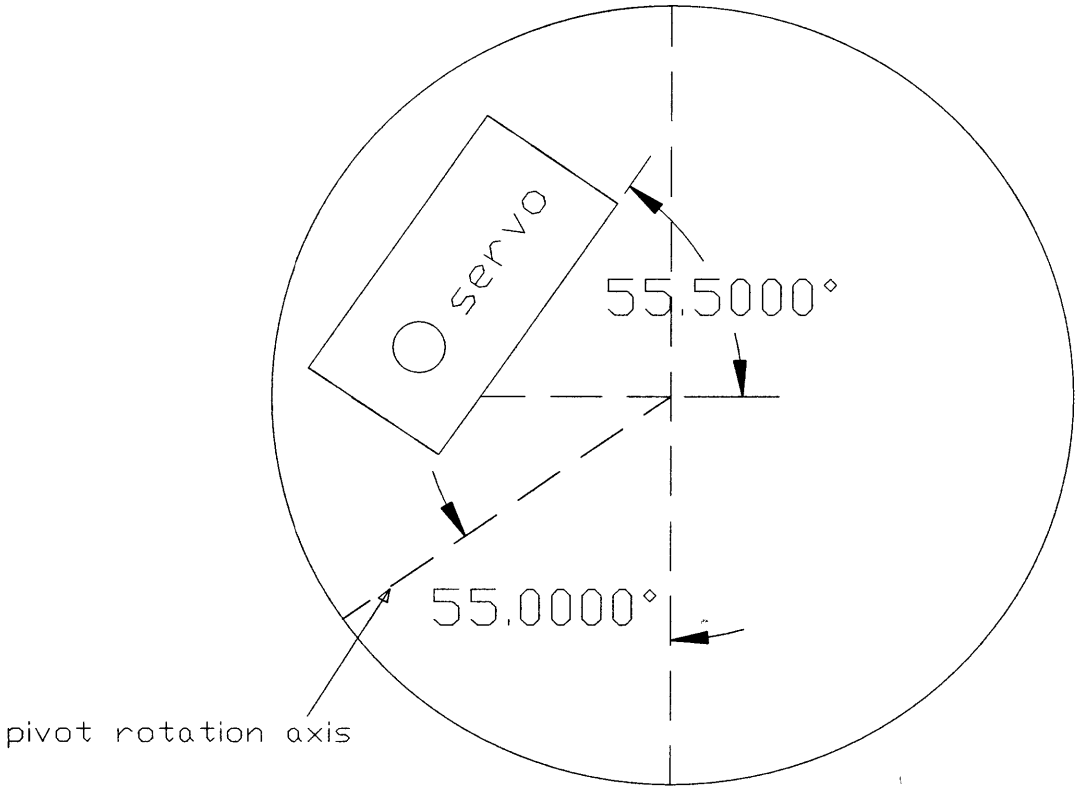

Figure 27: Positioning the Servo Inside the Tail Module

Since the servo only needs to rotate through 120°, the whole gear is not needed. Hence, the worm gear was cut as to only keep the necessary part. This cut worm gear is then attached to the pivot.

For assembly purposes, a section cut was performed at the back of the tail module. This separated the tail module into two. There is the main part with cavities where the servos and tails would fit, and then a cap which is screwed on to hold everything in place.

The cavities for the servos were then drawn with the right machining radii as was done with the test article. The placement of the servo inside the high-g vehicle can be seen in the next figure. (figure 28)

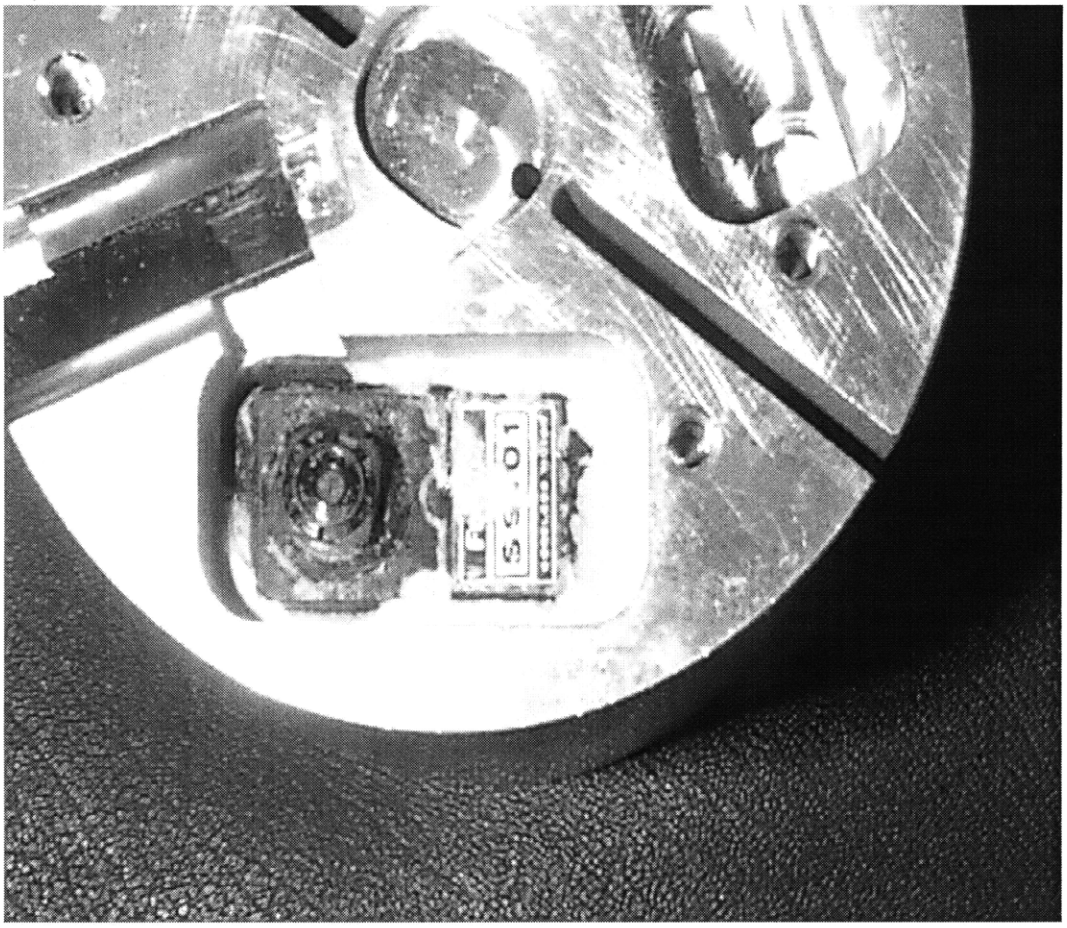

Figure 28: Servo Mounted Inside the Main Part of the Tail Module.
(with cap removed)

Propulsion Back-up Plan: Electric Motor

During the course of the year, the propulsion of the vehicle became one of the team's concerns. Investigation into a possible back-up plan became one of the author's responsibilities.

5.1 Defining the Need for a Back-up Plan

5.1.1 Initial Selection of the Means for Propulsion

A feasibility analysis was performed to decide which means of propulsion seemed optimal. Rockets, gas engines and electric motors were all considered.

The gas engines was eventually selected as the more promising solution. The main reason for rejecting the electric motor was that g-hardened batteries, able to deliver the large amounts of power required, were just too large. Use of an electric motor also greatly decreases the flight time.

5.1.2 Status of the Gas Engine Design

The possible engines selected for the final design were a two-stroke engine and a Wankel engine. An RC equivalent of each engine was tested in the Air Gun at Picatinny. The two-stroke engine was selected since it survived the 15,000 g acceleration while the Wankel engine did not. As already discussed, in addition to the engine, a glow plug, an engine starter mechanism, a servo for the carburetor and a gas tank are all needed. All these components have to be incorporated into the cone module.

5.1.3 Obstacles in Gas Engine Design

A few concerns surfaced about the gas engine. The first concern was whether or not the engine could start at an altitude of 7500 feet. RC engines usually have more trouble starting because of lack of oxygen and many attempts are required to get the engine started. It was therefore unknown if the engine could start especially since it has to start on the first try.

Another concern was the starting mechanism. One way to start the motor is to use a starter motor. This adds another component in the design since a battery to run the motor is now needed. Such a motor would require about 100 W. The battery for the electronics could not be used since

it could only give about 25W as a maximum power. A different battery would then have to be selected to allow for a maximum power draw of 100 W. G-hardened batteries able to provide this much peak power were too large. Hence the starter could not be used to start the engine. Another option was to use a torsional spring to start the engine. The spring would be pre-loaded to the propeller during assembly. When the propeller deploys, the spring is free to unwind, rotating the propeller enough to start the engine. This was the starting mechanism chosen, but uncertainties remained on whether or not the spring could rotate the propeller enough.

The last major concern about the gas engine is the large number of components that are needed. This creates a problem with both the space constraints and the overall reliability of the system. All of these engine components had to fit inside the cone module. The many different parts of the engine also reduce the reliability of the system. Indeed, since every component can fail they each reduce the reliability of the system.

5.1.4 Advantages of the Electric Motor

With an electric motor, only the motor and a battery are needed. This solves the space constraints and reliability concerns. The electric motor also starts when it receives the power from the battery. Hence, there no longer are any concerns about the starting mechanism or the altitude of deployment. Yet, the same initial concerns about the electric motor remain, notably battery size and flight time. After the successful tests of the servo motors, there was increased hope that an electric motor might work. At least two of the motors, from the servos tested, survived. These motors were not modified since no epoxy could be inserted inside. It seemed reasonable that a larger motor might also survive.

5.2 Electric Motor Selection

From last year's work by Ted Conklin[1], the most feasible motor company was Aveox since they were the only ones found to manufacture motors of small enough sizes giving the right power. Other companies were investigated, but they all manufactured motors that were too large for the application. Aveox motors were therefore selected. These motors are coreless motors with

1. Conklin, Theodore, *MIT/Drper Technology Development Partnership Project: Systems Analysis and On-Station Propulsion Subsystem Design*, Massachusetts Institute of Technology, Cambridge, MA, June, 1997

a fixed coil. A varying current is required at the input to get motion from the rotor. This requires a speed controller. This adds an extra component to the system.

The requirements from the electric motor are the same as those for the gas engine. The motor has to be able to provide 0.8 hp or 600W. This value is simply the drag multiplied by the cruise speed.

To select the right motor, worked initiated last year was continued. More detailed calculations were performed from the technical information available on the motors. In figuring out the performance of an electric motor, the motor selected and the batteries used to power the motor have to be taken into account. It was first assumed that the batteries used would be cells of Nickel Cadmium rechargeable batteries. This selection of battery will be justified in the following section of this chapter. The following procedure was performed to get the performance from a certain combination of battery and Aveox motor.

The characteristics available for each motor are:

1) the K_v constant in RPM/V, giving the slope of the RPM vs. voltage curve

2) the K_t constant in N.m/A, giving the slope of the torque vs. current curve

3) the internal resistance of the motor

4) the internal resistance of the speed controller. The internal resistance of the batteries was taken to be 0.0045 ohms per cell.

Knowing the current and voltage going into the motor, the motor's torque and speed is determined by:

$$T = K_t \times Ieff$$
$$w = K_v \times V_{eff}$$

This is a very simplified model for the motor since it does not take into account the mechanical load on the motor. The power output is then:

$$Pout = T \times w$$

The task is to find the current and voltage going into the motor. From the Kirchoff rule, the voltage and the current are related by the following:

$$V_{mot} = V_o - (n_{batteries} \times R_{battery} + R_{controller} + R_{motor}) \times I_{mot}$$

V_0 is the no load voltage across a battery which is 1.25 V for the Nickel Cadmium cell. This equation takes into account the voltage losses through the internal resistance of the batteries motor and controller. This creates a lower useful voltage available for the motor.

The electrical and mechanical quantities are related by the motor efficiency. Here a few assumptions have to be made to go on with the calculations. First the motor efficiency can be assumed to be 85%. This number is valid for a motor operating near its maximum efficiency. Another necessary assumption is that the efficiency losses are evenly distributed between losses in effective voltage and losses in effective current. This leads to the two following equations:

$$V_{eff} = \frac{V_{mot}}{\sqrt{0.85}}$$

$$I_{eff} = \frac{I_{mot}}{\sqrt{0.85}}$$

These six equations can be simplified to four equations by eliminating I_{eff} and V_{eff}. The five unknowns are V_{mot}, I_{mot}, P_{out}, T and w. The extra unknown is solved by adding a constraint to the output power. There is a speed controller for the motor which regulates the power going into the

motor. This constraint is set as: $P_{out} = 600W$. This constraint also serves as an empirical constraint to correct for the fact that the mechanical loading on the motor was ignored.

This system of equations can be solved using matrix algebra after having linearized the third equation. The solution is found by solving the following matrix equation:

$$A\vec{x} = \vec{b}$$

which has the solution:

$$\vec{x} = inv(A) \times \vec{b}$$

Since one of the equations had to be linearized to fit into a matrix, a few iterations will help to increase the precision. The best starting point for the iteration is $V_{mot} = V_o$, since not much of the no load voltage will be lost in the different internal resistances.

The Matlab file performing these operations can be found in Appendix B.

The motor manufacturer provided a program that calculates these same parameters in a similar fashion. The results from the two methods are usually within 10%. This algorithm has the additional advantage of providing a better estimate for the motor efficiency. This is important since some motor-battery selections will only provide the 600 W of output power in theory. In actuality, the power output of the motor at that power will be considerably less, because the efficiency is much less than 85%. Finally, this algorithm performs calculations taking into account torquing on the motor by the propeller. This is an important effect in defining the speed the motor will run at. This program was therefore used to do most of the calculations. Nevertheless, the preceeding equations in this chapter provide the reader with much of the assumptions used to make the calculations.

It is now possible to calculate the output characteristics of a multitude of motor-battery combinations. The results are set up in the following table.

Table 12: Motor Characteristics

Motor type	Power output(W)	Power inout(W)	Battery quantity	I_{max} (A)	V_{max} (V)	Motor eff.	Motor length(cm)	Diameter (cm)	Cost ($)
F10LMR	652	734	13	60.7	12.1	88.9	9.14	3.81	304.95
F16LMR	627	698	20	32	21.8	89.8	9.14	3.81	314.95
F27LMR	641	726	26	24.7	29.4	88.4	9.91	3.81	324.95
1412/5Y	618	737	21	32.2	22.9	83.9	6	3.73	209.95
1817/3Y	636	718	25	25.5	28.0	88.6	8.71	4.55	549.95
1415/4Y	610	714	20	32.9	21.7	85.5	6.75	3.73	239.95

The 1412Y/5Y was selected since it is the smallest of all the motors and it's current draw is not too large. It was also the cheapest motor being 20% cheaper than the 1415/4Y and 35% cheaper than the F16 LMR, which are the two motors that have very similar characteristics.

5.3 Battery Selection for Electric Motor

5.3.1 Battery Type Selection

As previously discussed, the battery has to provide 700W of power. This is greater than the motor's output power because of the efficiency of the motor. The only high-g batteries able to provide this much power are thermal batteries.These batteries can provide the high currents necessary for short periods of time. The short life of the batteries is not a concern. Considering the reduced efficiency of electric power, a shorter flight time is expected. The different thermal batteries that were possible candidates for the design are in the following table (table 13).

Table 13: Eagle Picher Thermal Batteries

	Voltage (V)	Current (A)	Power (W)	Max power duration (s)	g loading	pulse width (ms)	volume (cm^3)	mass (g)
EAP-12021	29	30	870	300	500	0.5	1245.4	3336.9
EAP-12051	30	9.2	276	630	4600	10	662.2	1779
EAP-12106A	75	4	300	250	-	-	579	1802
CAP-12115A	7	7	49	1.5	-	-	2.06	76.2
EAP-12141	50	7	350	300	63	3	637	2043
EAP-12145	30	16	480	120	-		249	644.7
EAP-12150	100	4.5	450	150	65	6	226	750
EAP-12155	27	13	351	200	7	50	201	590
EAP-12162	25	15.9	397.5	200	-	-	178.6	600
EAP-12167	30	5.75	172.5	1100	100	5	950	2290
EAP-12172	150	8	1200	150	400	-	363	1064
EAP-12185	90	2.8	252	80	48	30	70.5	900
EAP-12192	30	11	330	920	36	30	1176	3632
EAP-12198	28	18	504	100	470	200	170	581
STB-60V	70	7	490	180	100	-	334.6	-

It should be noted that most of these batteries were designed to specific requirements from a customer. Since none of these batteries were ever supposed to withstand accelerations comparable to that for the operational vehicle, none of these were tested or qualified to the desired specifications. During conversations with engineers from Eagle Picher, their main concern was the amplitude and the duration of the accelerations in the gun. They had never designed a battery with such requirements, and did not have the capabilities to perform tests under these conditions. These batteries are manufactured order by order. Hence, their cost is generally on the order of tens of thousand dollars. It was therefore too expensive to buy and test these batteries at Picatinny.

The next alternative was to select commercial batteries and test if they withstand the gun launch conditions. Realistically, a maximum of fifty cells can be put together to power the electric motor. Above that number, there are too many connections, and the reliability of the battery is too small. This means that each battery has to provide at least 15 W to obtain the 700 W that are necessary. The typical cell has a voltage of 1.5 volt which means the current draw is 10A. This is much more than the typical Duracell battery can give. The only batteries found to give that much current are again the Nickel Cadmium cells, which can deliver very high currents although the

practical limit is set at 30A. Hence, this battery was selected to eventually power the electric motor, which is why it was used to perform calculations in the preceeding section.

5.3.2 Cell Size Section.

The next step was to decide which configuration of cells was optimal. The goal was to find the cell size providing the largest power density of all Nickel Cadmium cells. The results are presented in the following table (table 14).

Table 14: Capacity of Nickel Cadmium Cells

Battery reference	Voltage (V)	Capacity (Ah)	diameter (mm)	height (mm)	Power density (Wh/cm^3)
N-1C	1.2	2.2	33	60	0.051
N-2U	1.2	1.4	26	50	0.063
N-3US	1.2	1	14.5	50	0.145
N-3U	1.2	0.7	14.5	50	0.102
N-4U	1.2	0.25	10.5	44.5	0.078
N-50AAA	1.2	0.05	10.5	16	0.043
N-1000SC	1.2	1	23	34	0.085
N-1300SC	1.2	1.3	23	43	0.087
N-2000C	1.2	2	25.8	50	0.092
KR-4400D	1.2	4.4	33	61.5	0.100
KR-7000F	1.2	20	43	146	0.113

The power density is calculated from:

$$Powerdensity = \frac{(Capacity \times Voltage)}{Volume}$$

It is apparent that the N-3US cell has the most efficient power density of all the cells. This means that by using a certain volume of cells, the longest run time for the motor will be obtained. With the combination of the 1412/4Ymotor and the 21 N-3US cells, the motor run time is a little over two minutes. This is to be added to the ten minutes of glide time.

5.4 Testing and Results

The next step was to test the motor battery combination in the Picatinny Air Gun along with the speed controller. The speed controller is the H60 which is used for motors powered by about twenty cells. To optimize the test, an extra Nickel Metal Hydride battery was tested. This battery could never be used for the motor because of its low power draw, but it was tested as a possible candidate to power the electronics.

To fit inside one air gun canister, the test article had to be separated in two. The motor and the two batteries fit into a larger test article. The speed controller was placed in a smaller article that was then placed on top of the test article in the canister.

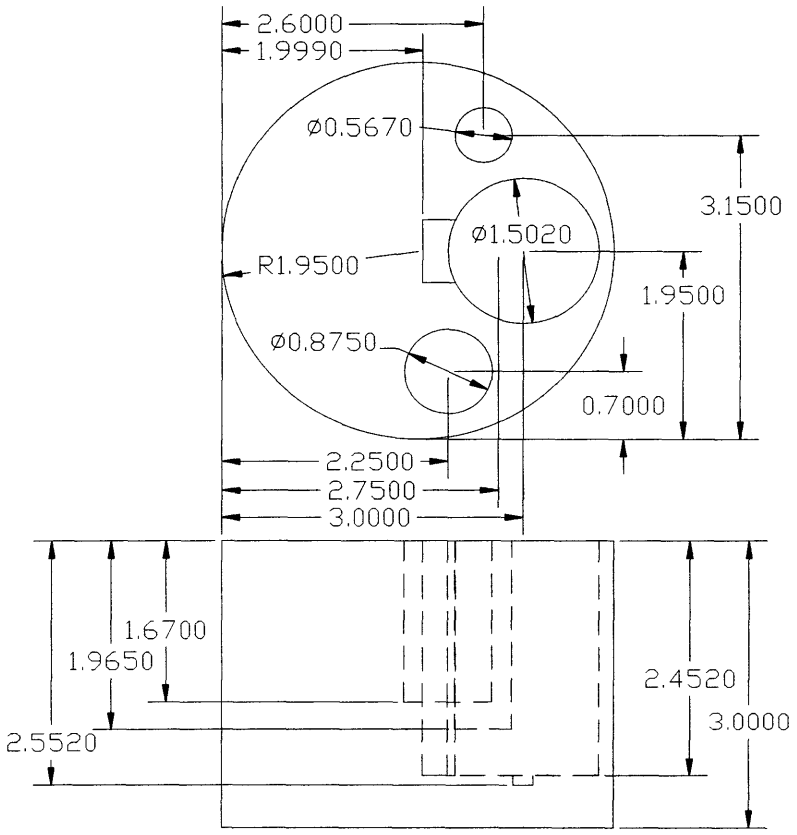

Figure 29: Test Article for Electric Motor

The motor fits in the larger of the three circular cavities, and the batteries are placed in the smaller of the cavities. No epoxy was used to g-harden the motor. Its casing has some holes, and the epoxy has a tendency to go everywhere. And since epoxy is not desirable inside the motor, it was not used. On the other hand epoxy was placed inside the cavities of the batteries.

The speed controller was g-hardened as the servos were, with epoxy keeping all the electronics in place. The drawing of the test article for the speed controller is in the following figure.

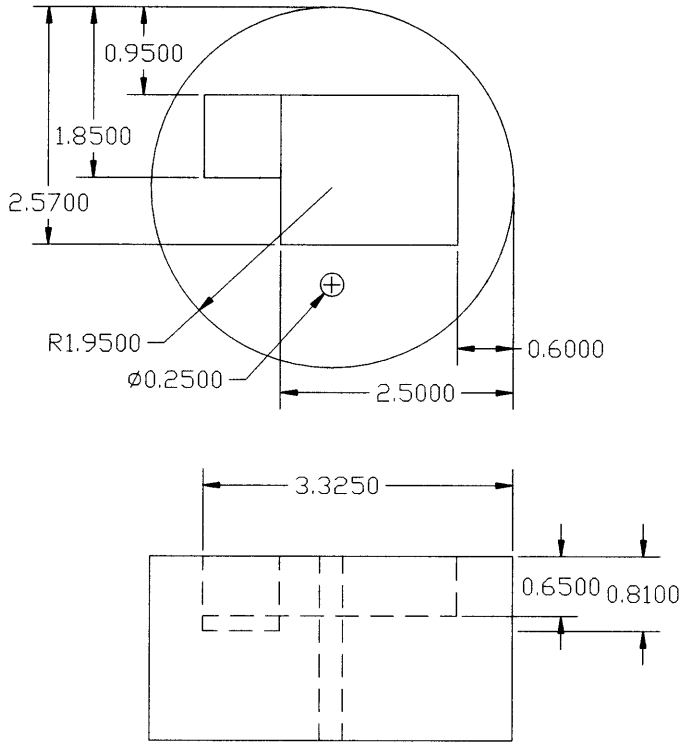

Figure 30: Test Article for Speed Controller

Both of these parts were machined out of aluminum and tested with their contents in the Air Gun. After the first test at 15000 g's neither the motor nor the battery survived. All the windings unwound due to the acceleration, and parts of the winding stuck out of the motor casing.

Since everything is packed so tightly inside the motor, it was unlikely that it could be g-hardened with epoxy. The battery had a zero

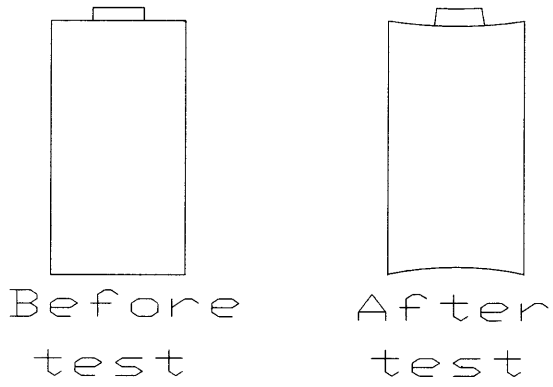

Figure 31: Illustration of Battery Test

voltage reading at the end of the test. Both sides of the battery had warped up, as can be seen in the illustration. This warping does not seem to be due to the mechanical structure of the battery. Instead it seems that some chemical reaction occurred during the gun launch, causing some small implosion. If this is the case, it is unlikely that anything can be done since it requires much knowledge about the chemical workings of a battery.

After this test, the back up plan for the propulsion was dropped.

Overall Testing Results

6.1 Testing of Individual Components

6.1.1 Tail Module Testing

For, the tail module, the only individual components tested were the servos as previously discussed, and two cameras. The two cameras tested were a pin-hole camera and a camera with a lens. Both of these cameras survived the air gun launches up to 15000g's. There was also a final air gun test of the complete tail module, with the tails, the servos and the gearing mechanism placed in their proper positions (figure 32). This test was successful except for a stress fracture in one of the servo's cavities. Only one of the servos was placed with epoxy for this sub-system test. The other servo cavity was left empty, and a crack developed. It was believed that the epoxy would have prevented this since the epoxy holds the servo and the cavity together.

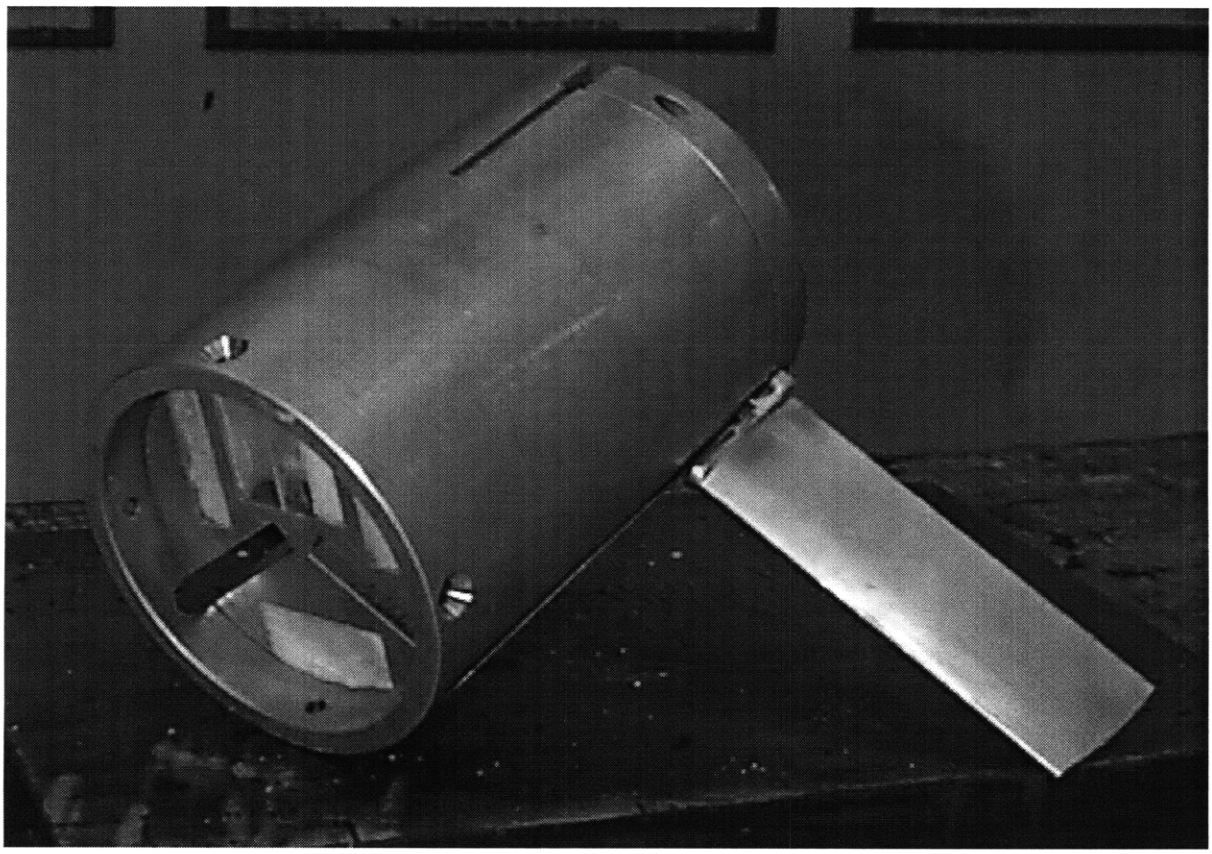

Figure 32: Tail Module Tested in Air Gun

6.1.2 Wing Testing

Different parts of the wing were tested in the air gun on different occasions. The first wing test consisted of just one section (figure 33). As the tests went along, design changes were performed to modify areas where the wings had failed. The final air gun test comprised of the whole wing and was a success.

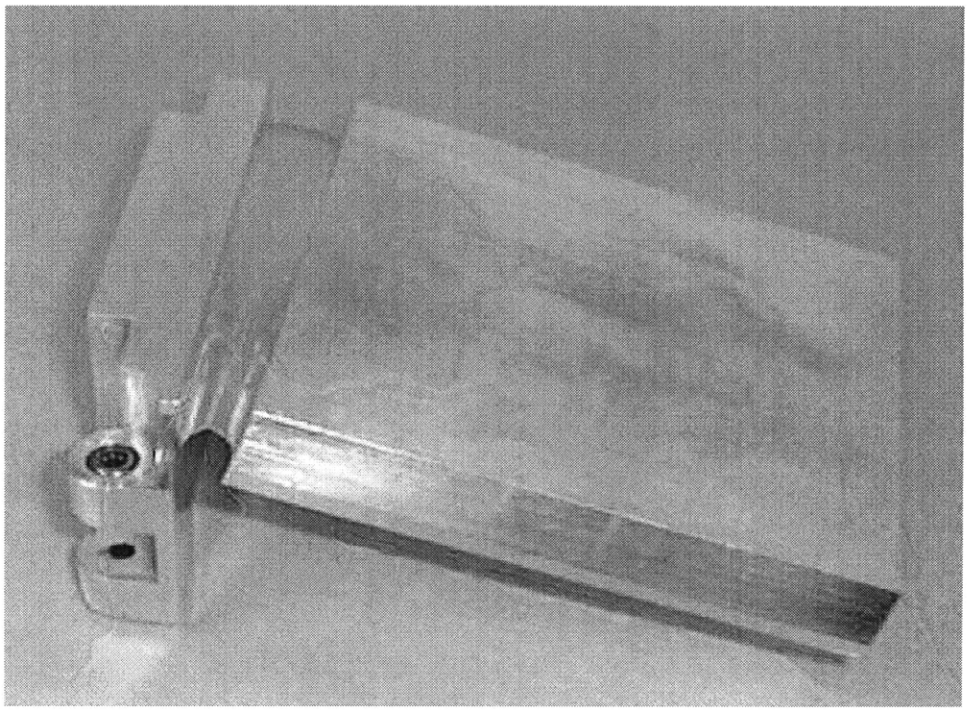

Figure 33: Wing Section Tested in Air Gun

The other wing test was a wind tunnel test to measure the aerodynamic performance of the wings, and mostly the drag of the wing-body combination. The lift to drag ratio was found to be ten.

6.1.3 Testing of other Components

Among the other components tested were engines. The two-stroke engine survived except for its carburetor. This engine was still incorporated into the design, since the carburetor would not have failed if it had been supported by some mechanical structure.

Tests were also performed with the parachute in the wind tunnel (figure 10). These tests were performed to study the deployment of the selected parachute. From these tests, it was decided to have the parachute attached to the flyer with a swivel joint to prevent the parachute from spinning.

6.2 System Testing

6.2.1 Flight Test Vehicle

At the completion of this thesis, the FTV was just a few days from its first flight. Hence, none of the results for the FTV test have been included in this thesis.

6.2.2 High-g Test

The high-g test was a canister test performed in a real gun at Dahlgren (figure 34).

Figure 34: Dahlgren Gun

To this extent, the shell with the flyer enclosed was assembled and placed inside a large canister (8"diametrer and 4' long, figure 35). This allowed for the verification of the survivability of individual components in the real gun environment. The structure of the system as a whole was also tested. During air gun tests, dummy weights would placed in the canister along with the test article to simulate the effect of the weight of the flyer that was in front. This was an approximate summation, and the real effect was tested at Dahlgren.

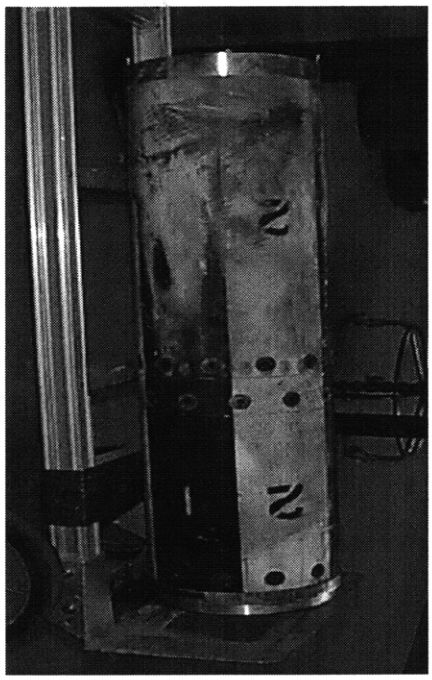

Figure 35: Canister after Dahlgren Test

The 14 May 1998 test was a success. Upon removal of the flyer from the shell, it was observed that the structure had not been compromised by the cannon launch. This was a very important result since it was the first test of the overall assembly, and the first involving rebound. As can be seen in figure 36, the flyer was deployable as before.

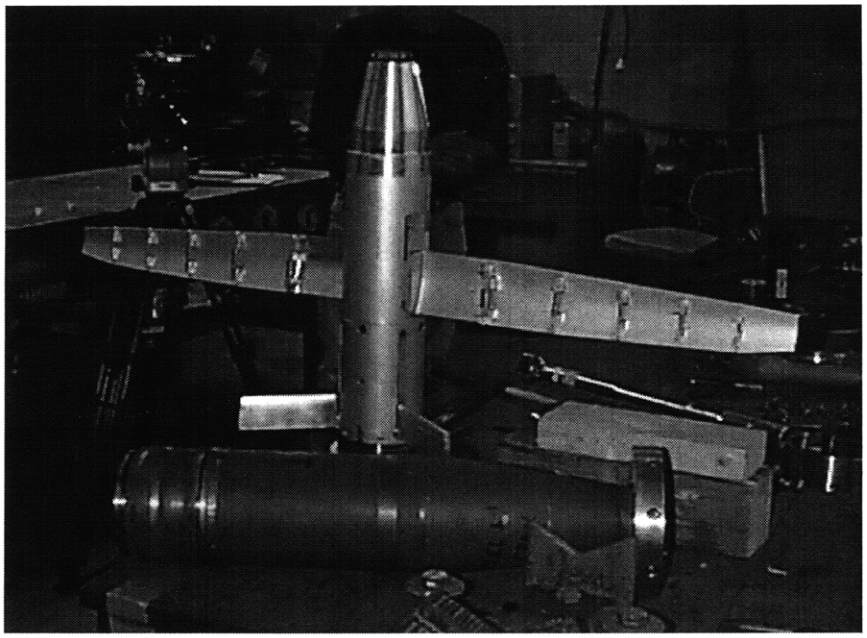

Figure 36: Flyer after Dahlgren Test

Conclusion

7.1 Lessons Learned

Here are a few of the most important lessons learned in this project.

- Use of Back-up Plans

Throughout the project, the necessity of having back-up plans was demonstrated. One such instance was when incorporating the worm gear system into the tail module for a Picatinny air gun test. It became apparent that the gears were not going to be delivered on time by the manufacturer. It was therefore useful to have had a few other backup plans, with other gears that could be incorporated into the design. Therefore, instead of scrambling to put together a new set of gears, one of the alternate set of gears was ordered. These new gears only required a few modifications in the design, and the test was performed as scheduled.

- Dependence on Suppliers

This brings up another of the lessons learned. When relying on suppliers for components, it is especially important to keep track of an order to insure that it arrives on time. If this is not done, it can lead to parts not being there when expected. This can lead to a delay in a test.

- Modularisation of the Design

The benefits of having a modularized design were also apparent. Having a modularized design, allowed for the concurrent design of different components to go on. For instance, the exact dimension of the wings did not have to be known for the design of the tail module or the propulsion system to be started. This reduced the number of iterations in the design.

- Use of StereoLithography

StereoLithography was a great asset in the design. During the design phase, having a solid model can be very helpful, and give a much better perspective than just having drawings. For instance, when trying to place the servos and the gearing mechanism, having the StereoLithogra-

phy model was very useful in visualizing where everything could fit, and how to orient different components.

7.2 Concluding Remarks

At the completion of this thesis, some of the concepts have been demonstrated, while other parts were yet to be tested. For the high-g test, the most important things that have survived were the wings, the tail along with their actuators, the propulsion module and the overall structure of the flyer. The flyer came out of the shell after the test in the same shape it was put into. (figure 37).

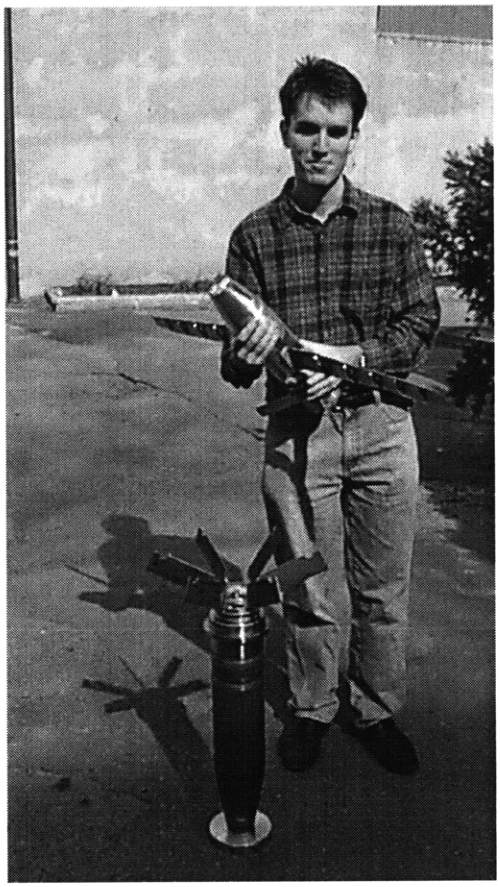

Figure 37: The Author Holding the Flyer before High-g Testing

It was proven that all the components in the high-g test vehicle could survive the high-g environment of the real gun. On the other hand, most of the deployment and the controls capabilities of the operational vehicle have yet to be proven. For the deployment, and other high-g vehicle characteristics, tests had not yet been performed. This includes the parachute pulling out the vehi-

cle from the shell, the stabilization fins at the back, the design of the power board and starting the engine. The power board design, and the fin stabilization are not as important since these are things that have already been done. So this effort concentrated on the "unobtainium" elements that could be addressed with the resources and time available.

Additional testing related to the FTV was going to be performed about one week following the completion of this thesis. This included demonstrating the aerodynamic performance, the auto-pilot, and the interfacing between the camera and the ground station.

APPENDIX A: Cavity Dimension Calculation from Tool Diameter Considerations

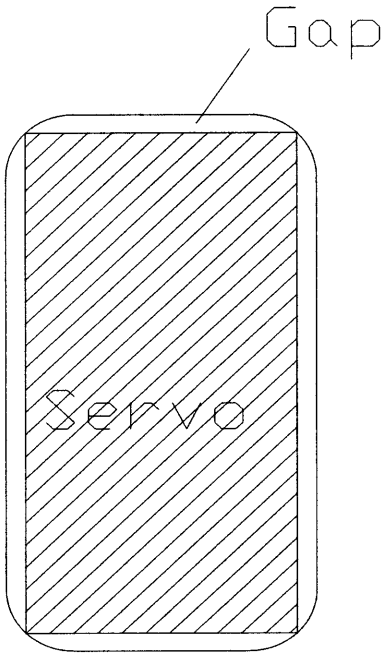

Figure 38: Illustration of Gap due to Tool Diameter

From geometry, the extra gap needed for a cavity as a function of the tool diameter used can be calculated. This is the distance d in the following drawing (figure 39).

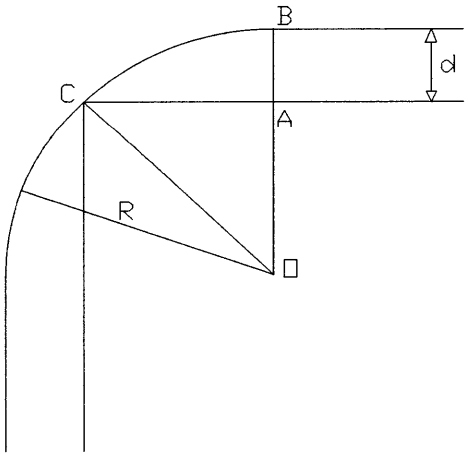

Figure 39: Drawing Used in Calculating Gap Size
(magnification of top left part of figure 38)

The gap size is d or the distance AB. It must be recognize that CO and BO are equal to the radius of the tool R. The triangle ACD is an Isosceles triangle with a right angle at A. In this triangle the following relation holds:

$$AO = \sqrt{\left(\frac{R^2}{2}\right)}$$

Then d =BO-AO and:

$$d = 0.293 \times R$$

This equation can be used for any mill bit to give the extra size that a cavity must be drawn to allow for non-square edges. It was used to design the final vehicle as well as in the manufacturing of all the different test articles.

APPENDIX B: Matlab File Computing Motor Output Characteristics

```
function x=motor(Kt,Kv,Rmot,n)

% This program computes and places the output power, the motor speed,
% the torque and the input voltage and current in the x vector

% it requires an input of the 2 motor constants as well as the motor
% resistance and number of batteries used

% x=[pout, w, T, V, I]

V0=1.25*n;
Rbat=0.0045;
Rcont=0.01;

%convert Kt from oz.in/A to N.m/A
Kt=Kt*7.06e-3
V1=V0
% converting Kv from RPM/V to (rad/s)/V
Kv=Kv*3.14159/30
for n=1:10


A=[0 0 1 0 -sqrt(0.85)*Kt
0 1 0 -sqrt(0.85)*Kv 0
1 0 -sqrt(0.85)*Kv*V1 0 0
0 0 0 1 (n*Rbat+Rcont+Rmot)
0 0 0 0 V1];
```

```
b=[0
0
0
V0
600/0.85];

x=inv(A)*b
end
P=x(1)
RPM=x(2)*30/pi
T=x(3)
V1=x(4)
I=x(5)
```

Appendix C: Technical Data Sheets of Components Used

PARAMETER	SUMMARY SPECIFICATION	
POWER REQUIREMENTS		
Input Supply Voltage	+ and - 15 VDC	
Input Power	7 watts	
PERFORMANCE	RATE CHANNELS	ACCELERATION CHANNELS
Standard Ranges	50, 100, 200, 500°/sec	1, 2, 5, 10 g's
Full Scale Output	±2.5 VDC	±7.5 VDC
Scale Factor Calibration (Factory Set)	<1%	<1%
Scale Factor Temp. Sensitivity	<0.03%/°C	<0.03%/°C
Bandwidth	>60 Hz	DC to >500 Hz
Linearity	<0.05% of FR	<25 µg/g²
Bias (Factory Set)	<2.0°/sec*	< ±12.5 mg
Temp Sensitivity (over full temperature)	<3°/sec from 25°C	<100 µg/°C
Long Term Stability (1 year)	<0.2°/sec*	<1,000 µg
G Sensitivity	<0.02°/sec/g	--
Alignment to Base (each axis)	<1°	<1°
Threshold Resolution	<0.004°/sec*	<10 µg
ENVIRONMENTS		
Operating Temperature	-40°C to +85°C	
Storage Temperature	-55°C to +100°C	
Vibration Survival	5 g rms, 20 to 2kHz random (1 minute duration	
Shock	200 g peak	
WEIGHT (nominal)	32 ounces	

*These specifications are dependent on the full scale ranges specified.

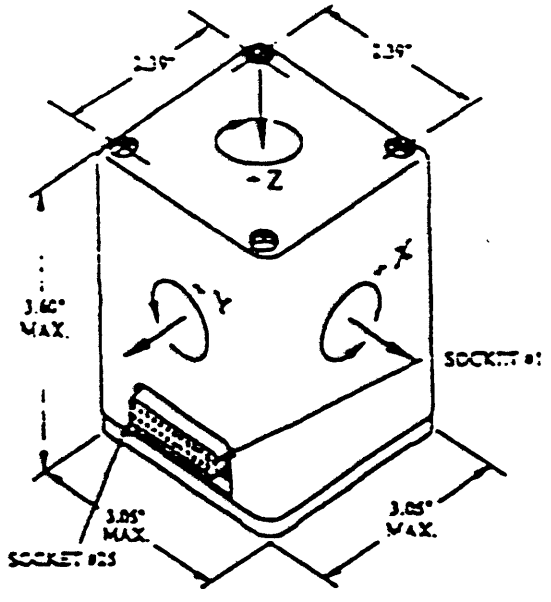

Connector Pin	Assignment
1	+15 VDC Input Power
2	-15 VDC Input Power
3	Power Ground
4	Case Ground
5	Rate-X Output
6	Rate-X Return
7	Rate-Y Output
8	Rate-Y Return
9	Rate-Z Output
10	Rate-Z Return
11	Accel-X Output
12	Accel-X Return
14	Accel-Y Output
15	Accel-Y Return
16	Accel-Z Output
17	Accel-Z Return
23	Temp Sensor Out (AD 590)
All other pins not used.	

D/A

1.2.7 PC/104 Module

PC/104 multimodule boards are small (3.550" x 3.775"), I/O or memory mapped boards which plug into a base board. The PC/104 boards connect to the PC/104 bus connector and convert the PC/104 bus signals to a defined memory or I/O interface. The PC/104 is a unique design approach to Embedded Systems users offering a broad range of expansion boards joined together on the PC/104 interface. The PCM-AIO is designed to fit on all WinSystems' processors that have PC/104 connectors, our LPM/MCM-SX386/486, and other CPU base boards.

1.3 SPECIFICATIONS

1.3.1 Electrical

A/D

Number of Channels:	Up to 8
A/D Resolution:	12-bits
Input range:	0 to +5 volts; single-ended -2.5 to +2.5 volts; differential
Coding:	Natural binary (unipolar) Two's complement (bipolar)
Nonlinearity:	1 LSB
Gain error:	Adjustable to zero
Conversion speed:	10 microseconds

D/A

Number of Channels:	2
D/A Resolution:	12-bits
Voltage Output:	0 to 5 VDC or -5 to +5 VDC
Output Drive:	2.5 mA

Power Requirements:

VCC	+5 VDC 5% at 10 mA (typ.)
VCC1	-12VDC 10% at 10 mA (typ.)
VCC2	+12VDC 10% at 10 mA (typ.)

DC/DC Converter

High Efficiency

Model exceeds 90 percent energy efficiency!

Features

- Clean and Filtered Power for the PC/104 bus.
- 5V&12V standard, -5V & -12V optional.
- "Load Dump" transient protection.
- 6 to 40 VDC input range, HE104.
- 25watt ouput, V104 & 50watt output, HE104.
- Stacks onto the PC/104 bus.
- 8 and 16 bit PC/104 versions.
- Highly compact, PC/104 compliant.
- AC bus termination available.
- -40 to 85C operation, HE104
- Low quiescent current.

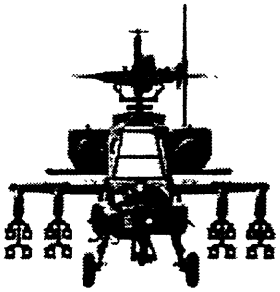

"High Performance"

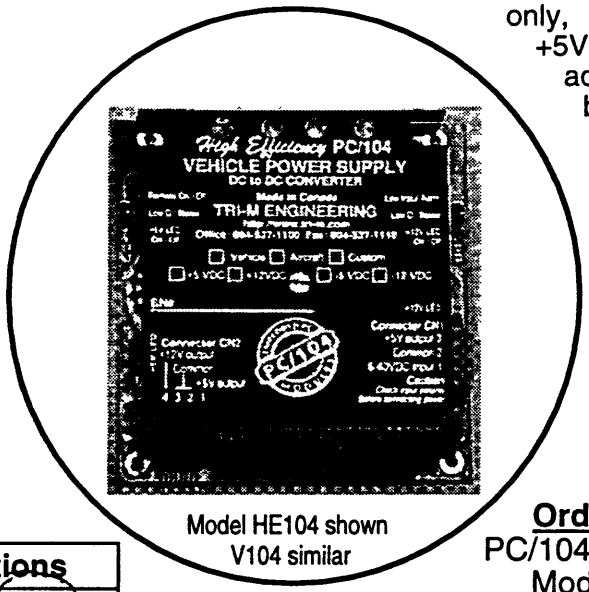

Model HE104 shown
V104 similar

HE104 and V104 General Description

Tri-M's PC/104 Vehcicle Power Supply is a DC to DC convertor. Both the HE104 and V104 provide a convenient means to supply power to PC/104 bus equipped products. The HE104 and V104 are designed for embedded vehicular applications and operate from a wide input range and have "Load Dump" and transient noise suppression on the power input.

The HE104 is a high efficiency, high performance convertor, with "logic level" remote shutdown, and 50 watt output capability. The HE104 is designed to withstand low ambient temperatures (-40C), and the shocks and vibration of mobile equipment.

The V104 is similar to the HE104, but supplies 25 watts, from an input range of 8 to 30 volts, and operates from 0 to 70C. The V104 also is designed to withstand shocks and high vibration.

The HE104 and V104 can be supplied +5VDC only, or can be supplied with both +5VDC and +12VDC outputs. In addition, -5VDC and -12VDC can be added to either version. This allows the use of PC/104 cards which normally require multiple power supply voltages, in a PC/104 system.

To improve PC/104 bus communication reliability, the HE104 and V104 can be ordered with "AC" bus signal termination. When supplied, both the 8 bit and 16-bit bus signals are terminated.

Power Supply Specifications

Model	HE104	V104
5V output*	10 A	5 A
12V output	2 A	1 A
-5V output	400mA	400 mA
-12V output	500mA	160 mA
Input Range	6 to 40V	8 to 30V
P-P Ripple*	<20mV	<50mV
Load Regulation **	<60mV	<30mV
Line Regulation **	±40mV	±40mV
Output temp. drift **	<40mV	<10mV
Efficiency	upto 95%	upto 85%
Temp Range	-40 to 85C	0 to 70C
Output Ripple	20mV**	50mV**
Temp Range	-40 to 85C	0 to 70C
Quiescent current	2mA***	22mA***
Size****	3.55"W. x 3.75"L x 0.6"Height	3.55"W x 3.75"L x 0.6"Height

Current rating includes current supplied to 12V, -12V, & -5V regulators.
*Measured on the 5V output.
**LEDs disabled, Low Quiescent mode enabled.
***Not including passthrough pins.

Ordering Information

PC/104 Vehicle Power Supply
Models HE104 &V104

Add the following suffixes to the model number:
"-5": 5VDC only "-8": 8bit PC/104 bus
"-512": 5&12VDC "-16": 16bit PC/104 bus
"-C": custom output "-N": no PC/104 bus
Example: HE104-5-16 (5VDC only with 16bit bus)

Optional -5V & -12V ouptputs:
- Specify HE104-OPT-N or V104-OPT-N where N=5 for -5V output, N=12 for -12V output and N=512 for both -5V and -12V outputs

Optional "AC" bus termination:
- Specify HE104-OPT-T or V104-OPT-T for AC termination